In-Depth Proteome Analysis of Arabidopsis Leaf Peroxisomes Combined with in Vivo Subcellular Targeting Verification Indicates Novel Metabolic and Regulatory Functions of Peroxisomes[1][W][OA]

Sigrun Reumann[2], Sheng Quan, Kyaw Aung, Pingfang Yang, Kalpana Manandhar-Shrestha, Danielle Holbrook, Nicole Linka[3], Robert Switzenberg, Curtis G. Wilkerson, Andreas P.M. Weber[3], Laura J. Olsen, and Jianping Hu*

Michigan State University-Department of Energy Plant Research Laboratory (S.R., S.Q., K.A., P.Y., K.M.-S., R.S., J.H.), Plant Biology Department (K.A., N.L., C.G.W., A.P.M.W., J.H.), and Biochemistry and Molecular Biology Department (C.G.W.), Michigan State University, East Lansing, Michigan 48824; and Department of Molecular, Cellular, and Developmental Biology, University of Michigan, Ann Arbor, Michigan 48109 (S.R., D.H., L.J.O.)

Peroxisomes are metabolically diverse organelles with essential roles in plant development. The major protein constituents of plant peroxisomes are well characterized, whereas only a few low-abundance and regulatory proteins have been reported to date. We performed an in-depth proteome analysis of Arabidopsis (*Arabidopsis thaliana*) leaf peroxisomes using one-dimensional gel electrophoresis followed by liquid chromatography and tandem mass spectrometry. We detected 65 established plant peroxisomal proteins, 30 proteins whose association with Arabidopsis peroxisomes had been previously demonstrated only by proteomic data, and 55 putative novel proteins of peroxisomes. We subsequently tested the subcellular targeting of yellow fluorescent protein fusions for selected proteins and confirmed the peroxisomal localization for 12 proteins containing predicted peroxisome targeting signals type 1 or 2 (PTS1/2), three proteins carrying PTS-related peptides, and four proteins that lack conventional targeting signals. We thereby established the tripeptides SLM> and SKV> (where > indicates the stop codon) as new PTS1s and the nonapeptide RVx_5HF as a putative new PTS2. The 19 peroxisomal proteins conclusively identified from this study potentially carry out novel metabolic and regulatory functions of peroxisomes. Thus, this study represents an important step toward defining the complete plant peroxisomal proteome.

Surrounded by single membranes, peroxisomes are small, ubiquitous eukaryotic organelles mediating a wide range of oxidative metabolic activities that vary by the species, cell type, and environmental conditions in which the organism lives (Beevers, 1979; Van den Bosch et al., 1992). Plant peroxisomes are essential to physiological processes such as lipid metabolism, photorespiration, and plant hormone biosynthesis and metabolism (Olsen and Harada, 1995; Zolman et al., 2000; Hayashi and Nishimura, 2003; Nyathi and Baker, 2006; Reumann and Weber, 2006). They are also essential for embryogenesis and play pivotal roles in plant responses to abiotic and biotic stresses (Lin et al., 1999; Hu et al., 2002; Schumann et al., 2003; Sparkes et al., 2003; Fan et al., 2005; Lipka et al., 2005; Desai and Hu, 2008). As additional functions are discovered for plant peroxisomes, a comprehensive inventory of peroxisomal proteins will be crucial to determine the underlying mechanisms for the new roles.

Because peroxisomes lack DNA, all peroxisomal proteins are imported directly from the cytosol or via the endoplasmic reticulum (ER; Purdue and Lazarow, 2001). With a few exceptions, proteins destined to the peroxisome matrix contain a conserved peroxisome targeting type 1 (PTS1) or type 2 (PTS2) signal. PTS1 is a tripeptide sequence located at the extreme C terminus of a majority of matrix proteins; it consists of SKL (Ser-Lys-Leu) or a variant of this canonical sequence. PTS2 is a nonapeptide sequence with the prototype RLx_5HL, which is present at or near the N terminus of some matrix proteins. After PTS2-containing proteins

[1] This work was supported by the National Science Foundation Arabidopsis 2010 Program (grant no. MCB 0618335 to J.H. and grant no. MCB 0618279 L.J.O.).

[2] Present address: Centre for Organelle Research, Faculty of Science and Technology, University of Stavanger, N–4036 Stavanger, Norway.

[3] Present address: Department of Plant Biochemistry, Heinrich-Heine-University, D–40225 Duesseldorf, Germany.

* Corresponding author; e-mail huji@msu.edu.

The author responsible for distribution of materials integral to the findings presented in this article in accordance with the policy described in the Instructions for Authors (www.plantphysiol.org) is: Jianping Hu (huji@msu.edu).

[W] The online version of this article contains Web-only data.

[OA] Open Access articles can be viewed online without a subscription.

www.plantphysiol.org/cgi/doi/10.1104/pp.109.137703

enter the peroxisome, the N-terminal domain is cleaved off in plants and animals (Purdue and Lazarow, 2001). In silico searches of fungal, plant, and animal genomes for proteins containing putative C-terminal PTS1 sequences revealed that plants may contain the highest number of peroxisomal proteins (Emanuelsson et al., 2003). Screening the Arabidopsis (*Arabidopsis thaliana*) genome for proteins carrying targeting signals specifically defined for higher plants (Hayashi et al., 1997; Reumann, 2004) has led to the identification of about 280 genes that encode proteins containing putative PTS1 (220) and PTS2 (60) peptides (Kamada et al., 2003; Reumann et al., 2004). Results from these in silico analyses suggest that, although only a few dozen proteins have annotated peroxisomal functions, the total number of proteins in plant peroxisomes may well exceed 300.

Novel plant PTS peptides are being discovered in the postgenomic era. The characterization of only three additional PTS1 tripeptides allowed the prediction of about 100 additional PTS1-containing proteins in Arabidopsis (Reumann et al., 2007). However, in silico predictions of peroxisomal proteins also have limitations. We are still unable to predict proteins that are targeted to the membrane of peroxisomes or imported into the peroxisomal matrix by non-PTS1/2 pathways or "piggy-backing" mechanisms. In addition, some true peroxisomal proteins are currently missed by predictions, because of our insufficient knowledge of PTS variant sequences. Furthermore, amino acid residues located adjacent to PTSs can be crucial in some cases for PTS recognition and peroxisome targeting (Brocard and Hartig, 2006). For example, protein targeting to plant peroxisomes by weak PTS1 tripeptides such as SHL> (where > indicates the stop codon) is dependent on the presence of basic residues upstream of PTS1 (Ma and Reumann, 2008); thus, plant proteins terminating with a weak PTS1 tripeptide and lacking essential targeting enhancer elements nearby are likely nonperoxisomal. In addition, proteins carrying strong PTS1s such as SKL> can be nonperoxisomal if the PTS1 is preceded by several acidic residues (Ma and Reumann, 2008). Lastly, some predicted PTSs may not be surface exposed and/or can be overruled by other targeting signals (Brocard and Hartig, 2006).

Mass spectrometry (MS) analysis of proteins from purified peroxisomes is a powerful alternative approach to discover peroxisomal proteins, especially those unidentifiable by computational strategies. To date, researchers have generally used two-dimensional gel electrophoresis (2-DE) of purified plant peroxisomes followed by MS analysis to identify proteins from peroxisomes taken from Arabidopsis green cotyledons and leaves (Fukao et al., 2002; Reumann et al., 2007) or from etiolated Arabidopsis and soybean (*Glycine max*) cotyledons (Fukao et al., 2003; Arai et al., 2008). Initial proteome analyses of Arabidopsis peroxisomes identified a relatively small number of proteins, largely due to the difficulty in isolating highly pure peroxisomes, which is a bottleneck in organelle proteomics (Fukao et al., 2002, 2003). A recent proteome study with improved peroxisome purification methods significantly increased the number of peroxisomal matrix proteins identified from leaf peroxisomes (Reumann et al., 2007). However, some known matrix proteins and unknown regulatory proteins, most membrane proteins, and numerous novel proteins predicted to be peroxisome targeted with high probability by in silico PTS searches (Reumann et al., 2004) remained undetected. Recently, Eubel et al. (2008) purified peroxisomes from Arabidopsis cell suspension cultures by free-flow electrophoresis and detected about 20 novel proteins whose functions had not been associated with peroxisomes before. One of these putative novel proteins was confirmed to be peroxisomal by in vivo subcellular targeting analysis (Eubel et al., 2008).

Because 2-DE has limitations in displaying hydrophobic, basic, and low-abundance proteins (Heazlewood and Millar, 2006), we employed a complementary one-dimensional gel electrophoresis (1-DE) approach to maximize the coverage of low-abundance peroxisomal proteins. In this in-depth proteome analysis of Arabidopsis leaf peroxisomes, besides 65 established plant peroxisomal proteins and 30 proteins that had been previously associated with peroxisomes only by proteomic data, we also identified 55 putative novel proteins of plant peroxisomes. By transiently expressing fusions between candidate proteins and yellow fluorescent protein (YFP), we confirmed the peroxisome assignment of 19 proteins discovered by proteomics, including 13 novel proteins identified, to our knowledge, for the first time in this study. Our study provides insights into potentially novel metabolic and regulatory functions of plant peroxisomes and exemplifies an important step toward uncovering the full proteome of this essential organelle.

RESULTS

High Coverage of Known Plant Peroxisomal Proteins

We isolated peroxisomes from 4-week-old Arabidopsis leaves using a previously established method (Reumann et al., 2007). To gain deeper insights into peroxisomal functions and identify low-abundance proteins, we used immunoblotting and silver-stained protein gel analysis to assess the purity of isolated leaf peroxisomes, followed by a 1-DE-liquid chromatography and tandem mass spectrometry (LC-MS/MS) strategy for protein identification.

Mitochondria and chloroplasts are known to partially copurify with leaf peroxisomes. The detection of plastidic proteins by available polyclonal antisera (e.g. those against the inner envelope membrane protein Tic110 and the stromal chaperone ClpC) was below detection limits when analytical protein quantities (5

μg) were used (data not shown). Mitochondrial contamination, however, could be detected by immunoblotting using a monoclonal antiserum against the 30-kD voltage-dependent anion-selective channel (VDAC) protein from maize (*Zea mays*; Fig. 1A). In addition, the intensity of the Arabidopsis VDAC band correlated with the abundance of a 110-kD protein band on silver-stained analytical SDS gels among different peroxisome isolates. The size of the protein indicated its identity as the P-subunit of the mitochondrial Gly decarboxylase, a major protein of leaf mitochondria (Fig. 1B; Supplemental Table S1). Using both immunoblotting and silver staining of protein gels as selection criteria, we identified three of approximately 30 preparations as leaf peroxisome isolates of highest purity and pooled these samples for subsequent proteome analysis. To increase the chance of discovering low-abundance proteins in the sample, we separated a large amount of peroxisomal proteins (500 μg) on a 1-D gel and cut the gel lane into 16 slices after electrophoresis (Fig. 1C). Proteins in each gel slice were in-gel digested by trypsin; the resulting peptide mixtures were subjected to LC-electrospray ionization-MS/MS. Proteins were judged to be present in the sample if they had a 95% probability of being correctly identified, as assigned by ProteinProphet (Nesvizhskii et al., 2003).

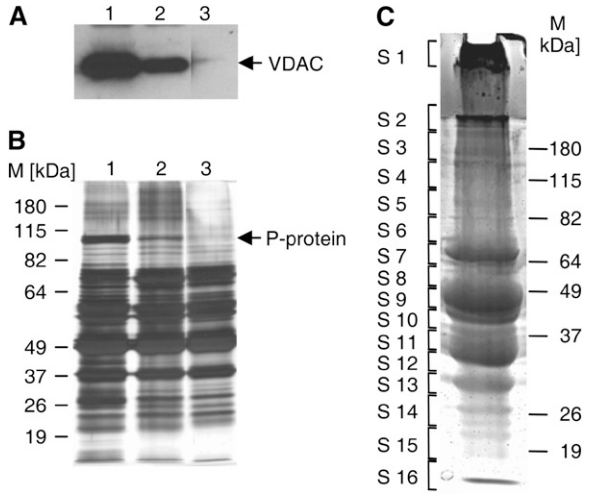

Figure 1. Purity analysis and 1-D gel separation of peroxisomal proteins. A and B, Leaf peroxisomal proteins (5 μg each lane) were separated on acrylamide minigels. Anti-VDAC immunoblotting (A) and silver staining (B) served to determine the relative contents of mitochondrial VDAC and the P-protein, respectively, while verifying the total amount of loaded proteins in parallel (B). According to the relative content of mitochondrial proteins, leaf peroxisome isolates were classified as of low (lane 1), moderate (lane 2), and high (lane 3) purity. All lanes in each panel are from the same gel. C, Leaf peroxisomal proteins (500 μg) of highest organelle purity were separated on a 10% SDS-PAGE minigel. After brief staining, the gel was cut into 16 slices and proteins were in-gel digested with trypsin and analyzed by LC-MS/MS. The line in S2 separates the stacking and resolving gels.

We identified 302 proteins, among which 280 had at least two matching peptides and 285 were detected by ≥99% probability (Table I; Supplemental Tables S1–S3). Sixty-five proteins are referred to in this study as established peroxisomal proteins, because they have been functionally characterized from at least one plant species. Except for seven proteins (ACX6, DEG15 protease, malate synthase, isocitrate lyase, polyamine oxidase 4, Hsp15.7, and sarcosine oxidase), we identified most matrix proteins that had been functionally characterized in plant peroxisomes (Supplemental Table S2). The 89% coverage (57 of 64 proteins) of established peroxisomal matrix proteins in this study is quite high compared with previous proteome analyses of plant peroxisomes. The coverage of membrane proteins in this study was also improved over a former study of leaf peroxisomes (Reumann et al., 2007). For example, all five members of the plant PEX11 family (PEX11a–PEX11e) of peroxisome proliferation promoters, the peroxisome biogenesis factor PEX14, two known metabolite transporters, PMP36 and PXA1, and MDAR4 (for monodehydroascorbate reductase isoform 4) were identified. Four of these 65 established peroxisomal proteins (ACX2, 4CLP2, PEX11b, and MDAR4; Supplemental Table S2) were identified for the first time in a proteomic study of plant peroxisomes.

We also identified 30 additional proteins whose peroxisomal association had been demonstrated previously only by proteome data and remained to be verified by an independent line of evidence (Table I; Supplemental Table S3). Twenty-two of these proteins had first been identified by Reumann et al. (2007), which included, for instance, nearly all of those with a proven or predicted role in pathogen and herbivore defense (e.g. BGL1, TGG1 and TGG2, and MIF; Table I), further supporting their putative peroxisomal associations. Eleven additional proteins first associated with peroxisomes by Reumann et al. (2007) were already confirmed to be peroxisomal by a subcellular targeting study of YFP fusion proteins (Reumann et al., 2007) and are now listed in the group of established plant peroxisomal proteins (Supplemental Table S2). Eight of the 30 proteins were independently identified by Eubel et al. (2008; ZnDH, AAE1, MCD, IndA, CuAO, AAE17, and PM-16) or Fukao et al. (2003; sT3).

Protein levels within a subcellular compartment can span a wide dynamic range. To compare the abundance of proteins discovered from our shotgun proteomic experiment, we calculated normalized spectral abundance factors (NSAFs; i.e. spectral counts that were normalized after taking into consideration protein size and variation between sample runs; Paoletti et al., 2006). Specifically, a spectral abundance factor (SAF) for each protein was first determined by dividing the spectral counts (i.e. the number of times a particular peptide from a given protein is sampled) of peptides assigned to this protein by the protein length. Then, each SAF was divided by the sum of SAFs from all proteins in the sample to generate the NSAF value

Table I. *Putative novel proteins of Arabidopsis leaf peroxisomes identified by 1-D LC-MS/MS and classified into functional groups*

Listed are 85 proteins, among which 30 had also been independently identified by previous proteome analyses (indicated in the Proteome Evidence column) but had not been confirmed to be peroxisomal by alternative methods. Functional categories 1 to 6 refer to β-oxidation (auxiliary), ROS metabolism, other metabolic enzymes, nucleotide and nucleic acid metabolism, chaperones and proteases, and other proteins, respectively. PTSs in parentheses, such as (SRF>) for At5g02240, indicate PTS-related peptides; SKV> in At4g16566.1 and SLM> in At5g65400.1 were later proven to be functional PTS1s in this study. Detailed biophysical and MS data on all these proteins are provided in Supplemental Table S3. Reu07, Reumann et al. (2007); Eub08, Eubel et al. (2008); Fukao03, Fukao et al. (2003); chpt, chloroplast; cyt, cytosol; nuc, nucleus; perox, peroxisome; pm, plasma membrane; n.d., not determined.

Gene Locus	Acronym	Annotation	Functional Category	PTS1/2	NSAF ($\times 10^{-3}$)	Proteome Evidence	EYFP Localization
At1g02920.1	GSTF7	Glutathione transferase	2	Unknown	0.54	This study	cyt
At1g04290.1	sT4	Small thioesterase isoform 4	1	SNL>	1.46	Reu07; this study	n.d.
At1g11840.1	GLX1	Glyoxalase I homolog	2	Unknown	0.40	This study	n.d.
At1g16730.1	UP6	Unknown protein	6	SKL>	0.70	This study	n.d.
At1g19570.1	DHAR1	Dehydroascorbate reductase	2	Unknown	0.53	This study	perox
At1g20010.1	TUB5	Tubulin β-5 chain	6	Unknown	0.13	This study	n.d.
At1g20560.1	AAE1	Acyl-activating enzyme 1	1	SKL>	0.31	Eub08; this study	perox
At1g26340.1	B5 #6	Cytochrome b_5, putative	6	Unknown	0.84	This study	n.d.
At1g45145.1	TRX-H-5	Thioredoxin H-type 5	6	Unknown	1.20	This study	n.d.
At1g48320.1	sT1	Small thioesterase 1	1	AKL>	2.54	This study	perox
At1g49240.1		Actin 8	6	Unknown	0.25	This study	n.d.
At1g50510.1	IndA	Indigoidine synthase A	3	RIx_5HL	2.58	Eub08; this study	perox
At1g52400.1	BGL1	β-Glucosidase 1	2	Unknown	1.13	Reu07; this study	n.d.
At1g52410.2	UP1/TSA1	Unknown protein 1/TSK-ASSOCIATING PROTEIN1	6	SSL>	0.97	Reu07; this study	n.d.
At1g64850.1		Calcium-binding EF-hand family protein	6	Unknown	0.35	This study	n.d.
At1g75750.1	GASA1	GA-responsive GAST1 protein homolog	6	Unknown	1.16	This study	n.d.
At1g77540.1	ATF2	Acetyltransferase	6	SSI>	0.50	This study	perox
At1g78300.1	GRF2	General regulatory factor 2, G-box-binding factor GF14 ω (14-3-3 protein)	6	Unknown	0.44	This study	n.d.
At1g78370.1	GSTU20	Glutathione transferase	2	Unknown	0.78	This study	n.d.
At1g78380.1	GSTU19	Glutathione transferase	2	Unknown	1.16	This study	n.d.
At2g05380.1	GRP3S	Gly-rich protein 3 short isoform	4	Unknown	n.d.	This study	n.d.
At2g16600.1	CYP19-1/ ROC3	Cyclophilin 19-1	5	Unknown	0.98	This study	n.d.
At2g21660.1	GRP7	Gly-rich protein isoform 7	4	Unknown	1.29	Reu07; this study	n.d.
At2g27490.1	COAE	Dephospho-CoA kinase	3	Unknown	0.24	This study	perox
At2g28760.1	UXS6	UDP-Xyl synthase 6	3	Unknown	0.17	This study	n.d.
At2g29590.1	sT5	Small thioesterase 5	1	SKL>	0.72	This study	perox
At2g30870.1	GSTF10/ ERD13	Glutathione transferase	2	Unknown	0.53	This study	cyt
At2g31670.1	UP3	Unknown protein 3	6	SSL>	1.83	Reu07; this study	n.d.
At2g36530.1	LOS2	Low expression of osmotically responsive genes 1	6	Unknown	0.38	This study	n.d.
At2g38540.1	LTP1	Nonspecific lipid transfer protein 1	1	Unknown	0.72	This study	cyt/pm
At2g41790.1	P-M16	Peptidase family M16	5	PKL>	0.85	Eub08; this study	n.d.
At2g42490.1	CuAO	Copper amine oxidase	3	SKL>	1.75	Eub08; this study	perox
At2g42520.1	RH37	DEAD-box RNA helicase 37	4	Unknown	0.18	Reu07; this study	n.d.
At2g42590.1	GRF9	General regulatory factor 9, G-box-binding factor GF14 μ (14-3-3 protein)	6	Unknown	0.22	This study	cyt/pm
At2g43940.1		Thiol methyltransferase	3	(STL>)	1.38	This study	n.d.
At2g47390.1		Ser-type endopeptidase	5	(SLL>)	0.03	This study	n.d.
At3g01980.1	SDRc	Short-chain dehydrogenase/reductase isoform c	1	(SYM>)	0.85	Reu07; this study	n.d.
At3g02360.1	6PGDH	Phosphogluconate dehydrogenase	1	SKI>	1.46	Reu07; this study	n.d.
At3g14150.1	HAOX1	Hydroxy-acid oxidase isoform 1	1	SML>	1.87	This study	perox[a]
At3g15950.1	UP2/NAI2	Unknown protein 2	6	(SLN>)	0.04	Reu07; this study	n.d.
At3g24170.1	GR	Glutathione reductase	2	(TNL>)	0.45	Reu07; this study	n.d.
At3g25530.1	GHBDH	γ-Hydroxybutyrate dehydrogenase	1	Unknown	0.29	This study	n.d.
At3g26420.1	ATRZ-1A	Gly-rich RNA-binding protein	4	Unknown	0.58	This study	nuc

(*Table continues on following page.*)

Table I. (*Continued from previous page.*)

Gene Locus	Acronym	Annotation	Functional Category	PTS1/2	NSAF ($\times 10^{-3}$)	Proteome Evidence	EYFP Localization
At3g48140.1	B12D1	Senescence-associated protein/ B12D-related protein	6	Unknown	0.64	This study	perox
At3g48170.1	BADH	Betaine aldehyde dehydrogenase	3	SKL>	4.90	Reu07; this study	n.d.
At3g51600.1	LTP5	Nonspecific lipid transfer protein 5	1	Unknown	0.24	This study	n.d.
At3g51660.1	MIF	Macrophage migration inhibitory factor	2	SKL>	4.05	Reu07; this study	n.d.
At3g55290.1	SDRd	Short-chain dehydrogenase/reductase isoform d	1	SSL>	1.82	Reu07; this study	n.d.
At3g56240.1	CCH	Copper homeostasis factor (copper chaperone)	5	(SQV>)	1.17	This study	cyt
At3g56460.1	ZnDH	Zinc-binding dehydrogenase	3	SKL>	6.84	Eub08; this study	perox
At3g56490.1	HIT3	His triad family protein 3	4	(RVx_5HF)	1.35	This study	perox/chpt
At3g61200.1	sT3	Small thioesterase 3	1	SKL>	0.90	Fukao03; this study	perox
At4g04320.1	MCD	Malonyl-CoA decarboxylase	1	SRL>	0.88	Eub08; this study	perox
At4g09320.1	NDPK1	Nucleoside diphosphate kinase type 1	3	Unknown	2.18	This study	perox/nuc/cyt
At4g14880.1	OASS A1	*O*-Acetylserine sulfhydrylase isoform A1	3	Unknown	0.26	Reu07; this study	n.d.
At4g16566.1	NBP/HIT1	Nucleotide-binding protein/His triad family protein 1	4	(SKV>)	3.11	Reu07; this study	perox
At4g17530.1	RAB1c	Ras-related small GTP-binding protein	6	Unknown	0.28	This study	nuc
At4g30010.1	UP8	Unknown protein	6	Unknown	0.63	This study	n.d.
At4g34870.1	CYP18-4/ ROC5	Cyclophilin 18-4	5	Unknown	1.98	This study	nuc/cyt/pm
At4g38740.1	CYP18-3/ ROC1	Cyclophilin 18-3	5	Unknown	0.66	This study	cyt
At4g39260.1	GRP8	Gly-rich repeat protein 8	4	Unknown	0.67	Reu07; this study	n.d.
At5g02240.1		Catalytic/coenzyme binding	3	(SRF>)	0.11	This study	nuc
At5g02500.1	Hsp70-1/ HSC70-1	Heat shock protein 70	5	Unknown	0.61	This study	n.d.
At5g10450.1	GRF6	General regulatory factor 6, G-box-binding factor GF14 λ (14-3-3 protein)	6	Unknown	1.14	This study	n.d.
At5g11910.1	ELT1	Esterase/lipase/thioesterase family isoform 1	1	SRI>	1.24	This study	perox
At5g15970.1	COR6.6	Cold-regulated protein (stress-induced protein KIN2)	6	Unknown	1.72	This study	n.d.
At5g16370.1	AAE5	Acyl-activating enzyme 5	1	SRM>	2.26	Reu07; this study	n.d.
At5g17920.1	METE1	Cobalamin-independent Met synthase	3	(SAK>)	0.78	Reu07; this study	n.d.
At5g20010.1		GTP-binding nuclear protein (RAN-1)	6	Unknown	0.26	This study	nuc
At5g23050.1	AAE17	Acyl-activating enzyme 17	1	SKL>	1.30	Eub08; this study	n.d.
At5g25980.1	TGG2	Myrosinase, thioglucosidase 2	2	Unknown	0.30	Reu07; this study	n.d.
At5g26000.1	TGG1	Myrosinase, thioglucosidase 1	2	Unknown	0.84	Reu07; this study	n.d.
At5g38480.1	GRF3	General regulatory factor 3, G-box-binding factor GF14 ψ (14-3-3 protein)	6	Unknown	0.56	This study	cyt/pm
At5g42980.1	TRX-H-3	Thioredoxin H-type 3	6	Unknown	1.20	This study	cyt
At5g43940.1	HMGDH	*S*-(Hydroxymethyl)glutathione dehydrogenase (GSH-FDH)	2	Unknown	0.37	Reu07; this study	n.d.
At5g44020.1		Acid phosphatase class B family protein	6	Unknown	0.94	This study	n.d.
At5g44250.1	UP5	Unknown protein	6	SRL>	0.63	This study	perox
At5g47040.1	Lon2	Lon protease homolog 2	5	SKL>	2.07	This study	perox[b]
At5g47210.1		Nuclear RNA-binding protein, putative	4	Unknown	0.08	This study	cyt/nonperox dots
At5g48230.1	ACAT2	Acetoacetyl-CoA thiolase 2	1	Unknown	2.11	Reu07; this study	n.d.
At5g48545.1	HIT2	His triad family protein 2	4	RLx_5HL	0.72	This study	perox
At5g54500.1	FQR1	Quinone reductase	3	(STA>)	0.28	This study	n.d.
At5g56030.1	Hsp90-2/ HSP81-2/ ERD8	Heat shock protein 81-2 (early responsive to dehydration 8)	5	Unknown	0.24	This study	n.d.
At5g59950.1		RNA and export factor-binding protein	4	Unknown	0.46	This study	n.d.
At5g65400.1	UP7	Unknown protein	6	(SLM>)	0.67	This study	perox

[a]C. Mayer and S. Reumann (unpublished data). [b]T. Johnson and L.J. Olsen (unpublished data; in vitro protein import assay and subcellular fractionation).

(Paoletti et al., 2006). In this study, all of those proteins detected by high NSAF values between 0.02 and 0.10 are established peroxisomal proteins, reflecting the predominance of photorespiratory and reactive oxygen species (ROS) metabolism-related enzymes in leaf peroxisomes (Fig. 2A; Supplemental Table S2). On average, the established peroxisomal proteins were identified by relatively high NSAF values (12×10^{-3}), whereas NSAF values for proteins that had been assigned to peroxisomes only by proteome data were about 7-fold lower (1.6×10^{-3}; Fig. 2, A and B). These data suggest that previous proteome studies allowed the identification of proteins whose abundance is 1 order of magnitude lower than that of most matrix enzymes identified by biochemical and genetic methods. However, given that we only performed a single proteomic experiment and that some limitations are associated with this quantification method (see "Discussion"), the NSAF-based data presented here only serve as a semiquantitative and tentative indication of protein abundance.

Assigning Putative Novel Proteins of Leaf Peroxisomes

In addition to the 95 peroxisomal proteins mentioned above, the higher sensitivity of our approach allowed the identification of a significant number of putative novel peroxisomal proteins. However, this achievement was inevitably accompanied by an increased identification rate of proteins from chloroplasts and mitochondria (Fig. 2, A and B), thus making the annotation of putative novel proteins of leaf peroxisomes more difficult. To differentiate between nonperoxisomal and putative novel peroxisomal proteins, we took advantage of the large number of organellar proteome studies published for Arabidopsis mitochondria and chloroplasts, summarized in the Arabidopsis Subcellular Proteomic Database

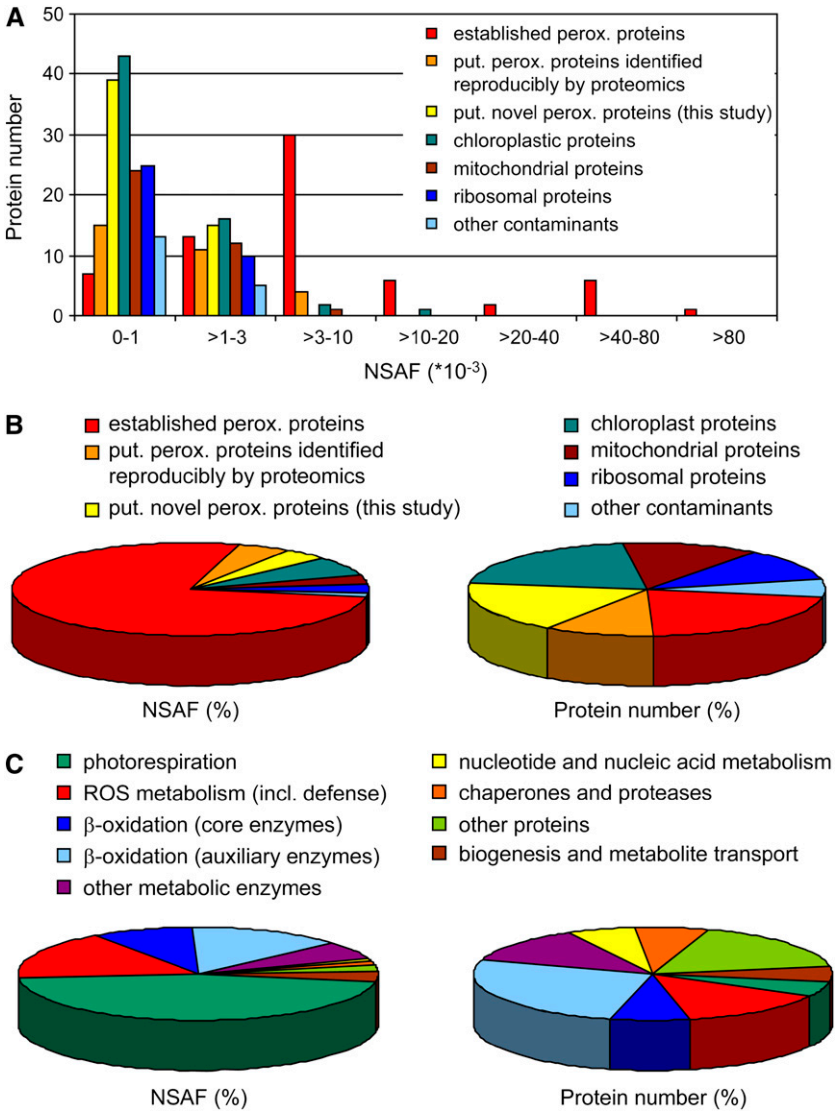

Figure 2. Subcellular and functional classifications of proteins identified in leaf peroxisomes. A, Number of peroxisomal and nonperoxisomal proteins grouped by NSAF values, which correlate with protein abundance. B, Relative abundance and protein numbers of peroxisome-associated and nonperoxisomal proteins. C, Functional assignment of peroxisome-associated proteins shown by relative abundance and protein numbers.

(www.plantenergy.uwa.edu.au/applications/suba2/; Heazlewood et al., 2007). We classified proteins rather stringently as nonperoxisomal contaminants (Supplemental Table S1) if they were identified from at least two organelle-specific proteome studies (for mitochondria and chloroplasts) or are known to be major constituents of other compartments (ER, cytosol, vacuole, or nucleus) or proteasomes. The quantity (percentage) of chloroplastic and mitochondrial proteins, based on their NSAF values, was 7.1% and 2.9%, respectively. Eukaryotic ribosomal proteins and a few ER proteins represented 3.1% and 0.6%, respectively, of the total NSAF values (Fig. 2, A and B), likely reflecting the association in biogenesis between peroxisomes and the rough ER. We also detected a few of the most abundant proteins from other subcellular compartments, including five cytosolic, three vacuolar, one nuclear, and three from proteasomes (Fig. 2, A and B; Supplemental Table S1).

Based on the above analyses, we concluded that 55 proteins have a strong probability for peroxisomal localization; thus, we referred to these proteins as putative novel proteins of leaf peroxisomes (Table I; Supplemental Table S3). Since the prediction of protein targeting to peroxisomes is not available at The Arabidopsis Information Resource (TAIR), most of these proteins were tentatively annotated as being cytosolic by TAIR for lacking identifiable organelle targeting signals. In contrast to the highly to moderately abundant proteins identified previously in leaf peroxisomes (see above), most putative novel proteins of plant peroxisomes detected for the first time in this study are of low abundance, with an average NSAF value of 0.77×10^{-3} (Fig. 2A). Forty-eight of these 55 proteins were identified with high confidence (≥99% probability), and 46 had at least two matching peptides for each protein. To verify the reliability of protein identification below the high-confidence threshold, five of nine proteins identified by one matching peptide and/or $95\% \leq x \leq 98\%$ probability (At5g02240, At5g47210, GRF9, ATF2, and B12D1; Table I; Supplemental Table S3; see below) were also chosen and subjected to subsequent in vivo targeting analysis. Nine of the putative novel proteins carry predicted plant PTS peptides defined previously (Reumann, 2004; Lisenbee et al., 2005; Reumann et al., 2007), seven contain PTS1/2-related sequences such as STL>, SLL>, SQV>, SLM>, and RVx_5HF, and 39 lack recognizable PTSs (Table I).

Functional Categories of the Novel Proteins

Based on annotation, sequence homology, and predicted function, we classified the putative novel proteins into several categories: β-oxidation (auxiliary enzymes), ROS metabolism (including glutathione metabolism and defense), other metabolic enzymes, nucleotide and nucleic acid metabolism, chaperones and proteases, and other proteins such as those with unknown functions (Table I).

A major functional group is composed of seven proteins with predicted auxiliary functions in fatty acid β-oxidation, four of which carry predicted PTS1s (Table I). Our study identified two additional members of the functionally uncharacterized family of small thioesterases (sTs). The predicted PTS1 (AKL>) for sT1 was previously shown to be highly conserved in homologous genomic sequences and plant ESTs (Reumann et al., 2004, 2007). Homologs of sT5, hydroxyacid oxidase isoform 1 (HAOX1), and esterase/lipase/thioesterase family isoform 1 (ELT1) in all or some of the plant lineages examined carry well-known major or minor PTS1 tripeptides, or PTS1-related sequences, such as CRM> and SLL> (Fig. 3, A–C), supporting the localization of these proteins in peroxisomes and indicating the conserved function for these proteins in peroxisomal metabolism across a wide range of plant species.

Enzymes with annotated functions related to ROS metabolism include four glutathione *S*-transferases (GSTs) that belong to the U and F subfamilies (GSTU19 and GSTU20, and GSTF7 and GSTF10). Dehydroascorbate reductase 1 (DHAR1) is probably the last missing protein of the peroxisomal ascorbate glutathione cycle (Jimenez et al., 1997), catalyzed by four matrix-targeted or membrane-associated enzymes (i.e. APX3, MDAR1/4, glutathione reductase, and DHAR). Peroxisomal DHAR had been characterized biochemically in pea (*Pisum sativum*) peroxisomes (Jimenez et al., 1997), but the corresponding cDNA had not been cloned from any plant species. Additional metabolic enzymes that are not obviously β-oxidation related include a thiol methyltransferase (At2g43940), a dephospho-CoA kinase homolog (COAE), UDP-Xyl synthase 6 (UXS6), nucleoside-diphosphate kinase type 1 (NDPK1), a catalytic/coenzyme-binding protein (At5g02240), and a quinone reductase (FQR1); three of these six proteins carry C-terminal PTS1-related tripeptides: STA> (FQR1; At5g54500), STL> (At2g43940), and SRF> (At5g02240).

In fulfillment of our intention to identify regulatory proteins, more than 20 of the putative novel proteins can be categorized as nonmetabolic proteins that most likely have regulatory roles in metabolism, signal transduction, or protein processing. Three proteins are likely involved in protein/peptide processing or turnover. Lon protease homolog 2 (Lon2) is orthologous to proteases from mammalian and yeast peroxisomes (Kikuchi et al., 2004; Aksam et al., 2007) and carries a conserved PTS1 (Fig. 3D). The Ser-type endopeptidase (At2g47390) has been detected in recent plastidic proteome studies (Kleffmann et al., 2004; Peltier et al., 2006; Zybailov et al., 2008). However, we classified this protein as a putative dual-targeted novel protein of peroxisomes due to its C-terminal PTS1-related peptide, SLL>, and the accumulation of upstream basic residues (KLRRSLL>). We also detected specific homologs of Arabidopsis chaperone families, including members of the heat shock protein 70 (HSP70) and HSP90 families, and three cyclophilin

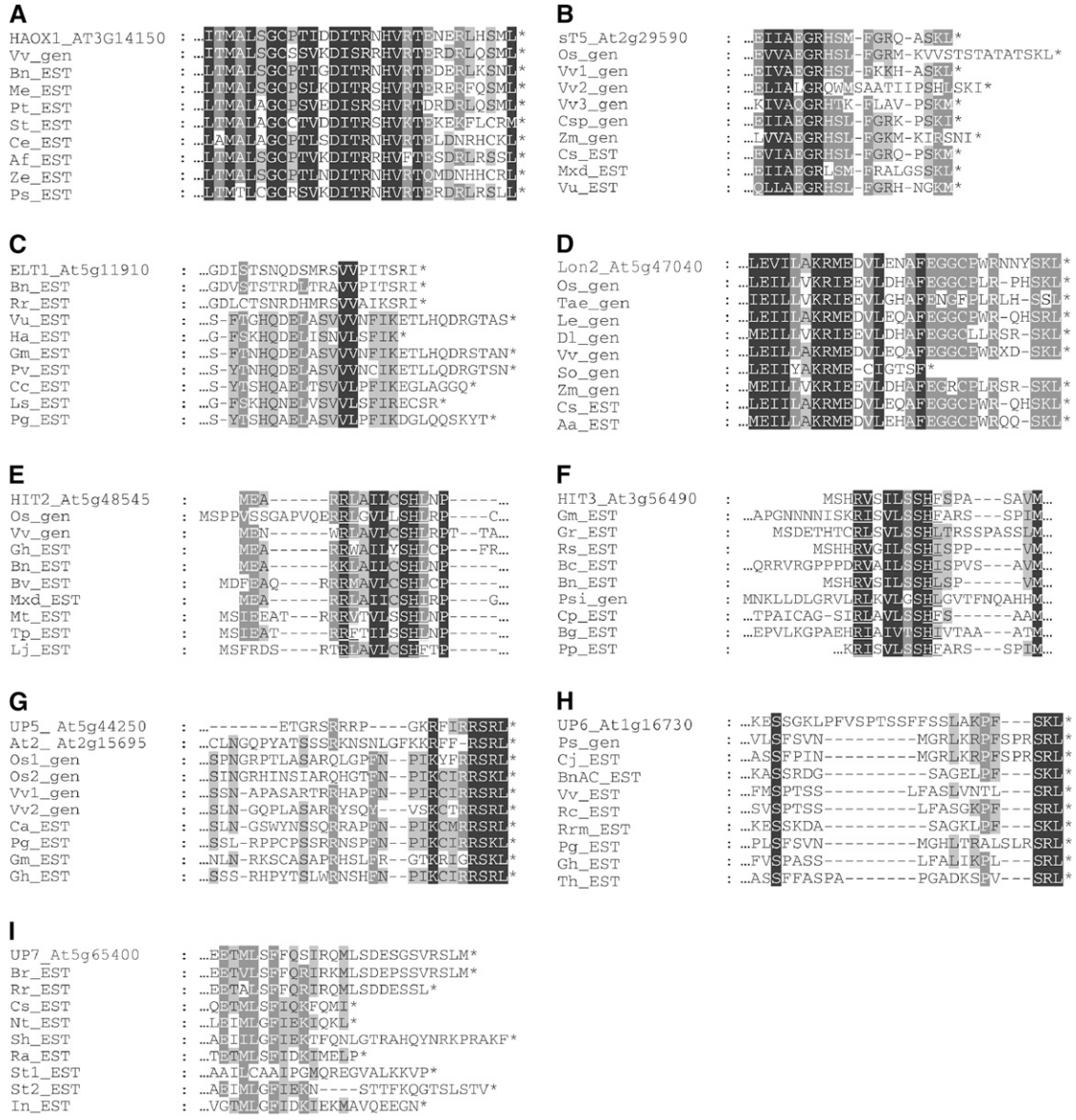

Figure 3. Analysis of PTS conservation in homologous plant ESTs for putative novel proteins. Asterisks indicate stop codons. Plant species abbreviations are defined in Supplemental Document S1.

(CYP) homologs. The copper homeostasis factor (CCH) is a putative copper chaperone with the C-terminal PTS1-related tripeptide SQV>.

In the category of nucleotide and nucleic acid metabolism, we uncovered two isoforms of the Gly-rich RNA-binding family of proteins (GRPs) that added to the two GRPs previously identified by Reumann et al. (2007), an RNA- and export factor-binding protein and a putative nuclear RNA-binding protein. In addition to the previously identified nucleotide-binding protein NBP (At4g16566; Reumann et al., 2007), which is now annotated as a member of the His triad protein (HIT) family (NBP/HIT1; Table I), two additional HIT family members (HIT2 and HIT3) were identified from this study. HIT2 carries a predicted and conserved PTS2 nonapeptide (RLx_5HL; Fig. 3E), and HIT3 contains an N-terminal PTS2-like nonapeptide that is also conserved among its homologs in other plant species (RVx_5HF; Fig. 3F). HIT proteins constitute a superfamily of nucleotide-binding and -hydrolyzing enzymes (Brenner, 2002). Arabidopsis contains five HIT domain-containing proteins, none of which has been functionally characterized.

Additional proteins with predicted regulatory functions include an acid phosphatase class B homolog, four isoforms of the 14-3-3 protein family of phosphorylated protein-binding factors (general regulatory factors), two thioredoxin homologs (TRX-H-3/5), two

GTP-binding proteins, and a second homolog of the peroxisomal acetyl transferase (ATF2). Furthermore, a gibberellin-responsive GAST1 protein homolog, a cold-regulated protein, a putative cytochrome b_5 homolog, and a senescence-associated protein (B12D1) were also assigned to this group. Homologs of actin and tubulin were also detected but were not associated with specific gene models, due to high sequence identity among the paralogs. Lastly, a few proteins lacking functional annotations are referred to as unknown proteins (UPs), among which three proteins carry predicted PTSs (UP5 [SRL>] and UP6 [SKL>]) or PTS1-related tripeptides (UP7 [SLM>]). Contrary to PTS1 conservation in UP5 and UP6 homologs across diverse plant families, peroxisome targeting of UP7 may be restricted to the Brassicaceae (Fig. 3, G–I).

Verification of Peroxisome Targeting by Fluorescence Microscopy

To validate peroxisomal targeting of the putative novel proteins identified in this proteome analysis, we tested the subcellular localization of a subset of these proteins utilizing in vivo targeting analysis of YFP fusions. During the course of this work, HAOX1 and Lon2 were independently confirmed by alternative methods to be peroxisome targeted (C. Mayer and S. Reumann, unpublished data; T. Johnson and L.J. Olsen, unpublished data; Table II) and therefore were excluded from further analysis. We divided the proteins into three categories based on the detection of predicted PTSs, PTS-related peptides, or no recognizable PTSs in these proteins and focused on representatives from each category.

The first group contained all seven putative novel proteins with predicted PTS1/2 (sT1, sT5, ELT1, ATF2, HIT2, UP5, and UP6; Table I), as well as eight PTS-containing proteins also identified independently by Eubel et al. (2008; AAE1, AAE17, MCD, ZnDH, CuAO, IndA, and P-M16) or Fukao et al. (2003; sT3) but whose peroxisomal localization had not been verified by alternative means (Table I). In fact, these eight proteins are also highly likely to be peroxisomal, because their homologs in some or all other plant species contain PTS or PTS-related sequences (see Reumann et al., 2007, for sT3; see Supplemental Fig. S1 for the other seven). The second group included four putative novel proteins with C-terminal PTS1-related sequences or N-terminal PTS2-related sequences, namely, the putative copper chaperone CCH (SQV>), a putative coenzyme-binding protein (At5g02240; SRF>), UP7 (SLM>), and HIT3 (RVx_5HF). We also added to this group HIT1/NBP (SKV>), another His triad family protein besides HIT2 and HIT3, because this protein had been identified previously through proteomics (Reumann et al., 2007) but had not been confirmed for its peroxisomal localization by alternative methods. The third group consisted of 16 putative novel proteins lacking predicted PTSs (Table II), most of which have annotated functions not associated with peroxisomes previously.

For medium-throughput cloning of candidate genes, we first created two Gateway-compatible destination vectors for fusion of the coding regions of candidate cDNAs to the N terminus (for PTS2-containing proteins) or the C terminus (for PTS1-containing proteins) of the enhanced YFP and for driving gene expression by the cauliflower mosaic virus *35S* promoter. Genes encoding proteins without predicted PTSs were cloned into both vectors or first into the vector for PTS2-containing proteins, because PTS2-related sequences are more difficult to detect than PTS1-like sequences. We were unable to clone AAE17, P-M16, and UP6 into destination vectors. As a result, YFP fusions for 33 genes (Table II) were transiently coexpressed with the peroxisomal marker gene *CFP-PTS1* in tobacco (*Nicotiana tabacum*) leaves. Subcellular protein targeting was analyzed by confocal laser scanning microscopy (CLSM) 2 to 3 d after *Agrobacterium tumefaciens*-mediated infiltration of the constructs.

All 12 proteins with predicted PTS1 or PTS2 peptides were verified to be targeted to peroxisomes, largely with one-on-one colocalization between their YFP fusions and the CFP-PTS1 peroxisome marker (Fig. 4). Notably, seven of these proteins (AAE1, ELT1, MCD, sT1, sT3, sT5, and ZnDH) have annotated functions in lipid metabolism (Table II).

Peroxisomal targeting for three of the five proteins with PTS-relative peptides was also confirmed. Of the four proteins with PTS1-related sequences, HIT1/NBP (SKV>) and UP7 (SLM>) localized to peroxisomes (Fig. 5, A and D), whereas CCH (SQV>) and At5g02240 (SRF>) were found to localize to the cytosol and nucleus, respectively (Table II). Peroxisome targeting of HIT1/NBP and UP7 suggested that SKV> and SLM> may be new PTS1 tripeptides. To further test this hypothesis, we analyzed the localization of two fusion proteins lacking the respective tripeptides. As expected, the truncated proteins failed to target to peroxisomes (Fig. 5, B and E). We also examined the subcellular localization of YFP with SKV> or SLM> fused to its C terminus (YFP-SKV or YFP-SLM) and observed strong colocalization of the respective fusion proteins with CFP-PTS1; in both cases, targeting to the nucleus and cytosol was also observed (Fig. 5, C and F). Besides UP7 and HIT1, the Arabidopsis genome contains 10 more proteins terminating with SLM> and 13 additional proteins containing C-terminal SKV>; these proteins thereby emerge as putative peroxisomal matrix proteins (Supplemental Table S4). Collectively, our results identified both SKV> and SLM> as new PTS1 tripeptides and suggested that some Arabidopsis proteins containing these two tripeptides may potentially target to the peroxisome as well.

HIT3, which has a PTS2-related nonapeptide (RVx_5HF) in its N-terminal domain, targeted to spherical structures labeled by CFP-PTS1 (Fig. 6A). Interestingly, this protein seems to be dual targeted, as reticulate structures mostly surrounding the chloro-

Table II. *Subcellular targeting results for selected proteins identified from this proteomic study*

chpt, Chloroplast; cyt, cytosol; perox, peroxisome; nuc, nucleus; pm, plasma membrane; TMs, transmembrane domains. Numbers in parentheses (on the scale of 0 to 1) are probabilities for the prediction of respective transmembrane domains by the plant membrane protein database Aramemnon (http://aramemnon.botanik.uni-koeln.de/); values greater than 0.7 were considered to be positive.

Gene Locus	Acronym	Annotation	PTS	Localization	Predicted TMs
Proteins with predicted PTS1s					
At1g20560[a]	AAE1	Acyl-activating enzyme 1	SKL>	perox	0
At1g48320	sT1	Small thioesterase 1	AKL>	perox	0
At1g77540	ATF2	Acetyltransferase	SSI>	perox	0
At2g29590	sT5	Small thioesterase 5	SKL>	perox	0
At2g42490[a]	CuAO	Copper amine oxidase	SKL>	perox	0
At3g14150[b]	HAOX1	Hydroxy-acid oxidase isoform 1	SML>	perox	0
At3g56460[a]	ZnDH	Zinc-binding dehydrogenase	SKL>	perox	0
At3g61200[c]	sT3	Small thioesterase 3	SKL>	perox	0
At4g04320[a]	MCD	Malonyl-CoA decarboxylase	SRL>	perox	0
At5g11910	ELT1	Esterase/lipase/thioesterase isoform 1	SRI>	perox	0
At5g44250	UP5	Unknown protein	SRL>	perox	0
At5g47040[d]	Lon2	Lon protease homolog 2	SKL>	perox	0
Proteins with predicted PTS2s					
At1g50510[a]	IndA	Indigoidine synthase A	RIx$_5$HL	perox	0
At5g48545	HIT2	His triad family protein	RLx$_5$HL	perox	0
Proteins with PTS-related peptides					
At3g56240	CCH	Copper homeostasis factor	SQV>	cyt	0
At4g16566[e]	HIT1/NBP	His triad family protein	SKV>	perox	0
At5g02240		Catalytic/coenzyme binding	SRF>	nuc	0
At5g65400	UP7	Unknown protein	SLM>	perox	0
At3g56490	HIT3	His triad family protein	RVx$_5$HF	perox/chpt	0
Proteins lacking recognizable PTSs					
At1g02920	GSTF7	Glutathione transferase		cyt	0
At1g19570	DHAR1	Dehydroascorbate reductase		perox	0
At2g27490	COAE	Dephospho-CoA kinase		perox	0
At2g30870	GSTF10/ERD13	Glutathione transferase		cyt	0
At2g38540	LTP1	Nonspecific lipid transfer protein		cyt/pm	0
At2g42590	GRF9	General regulatory factor 9 (14-3-3)		cyt/pm	0
At3g26420	ATRZ-1A	Gly-rich RNA binding		nuc	0
At3g48140	B12D1	Senescence-associated/B12D-related		perox	1 (0.74)
At4g09320	NDPK1	Nucleoside diphosphate kinase type 1		perox/nuc/cyt	0
At4g17530	RAB1c	RAS-related small GTP-binding		nuc	0
At4g34870	CYP18-4/ROC5	Cyclophilin 18-4		nuc/cyt/pm	0
At4g38740	CYP18-3/ROC1	Cyclophilin 18-3		cyt	0
At5g20010	RAN-1	GTP-binding nuclear protein		nuc	0
At5g38480	GRF3	General regulatory factor 3 (14-3-3)		cyt/pm	0
At5g42980	TRX-H-3	Thioredoxin H-type 3		cyt	0
At5g47210		Putative nuclear RNA-binding protein		cyt/nonperox dots	0

[a]These proteins were also identified by Eubel et al. (2008). [b]This protein was confirmed to be peroxisomal by C. Mayer and S. Reumann (unpublished data). [c]This protein was also identified by Fukao et al. (2003). [d]This protein was confirmed to be peroxisomal by T. Johnson and L.J. Olsen (unpublished data). [e]This protein was also identified by Reumann et al. (2007).

plasts were also labeled by yellow fluorescence (Fig. 6B). Thus far, three of the five Arabidopsis HIT proteins have been found to be associated with peroxisomes, revealing the unique involvement of this class of nucleotide hydroxylases/transferases in plant peroxisome functions.

We also tested the localization of 16 proteins that lack recognizable PTSs. Consistent with its predicted involvement in the peroxisomal ascorbate glutathione cycle, DHAR1 localized strongly to peroxisomes (Fig. 7A). COAE localized to the periphery of peroxisomes, suggesting its possible association with the membrane of these organelles (Fig. 7B). B12D1, a senescence-associated small protein of 88 amino acids, targeted to peroxisomes and led to peroxisome aggregation (Fig. 7C). This peroxisomal phenotype indicates that B12D1 may have a role in peroxisome distribution; alternatively, the phenotype may represent a dominant negative effect caused by attaching the 27-kD YFP to a small protein. Finally, NDPK1 was highly enriched in peroxisomes, paralleled by its weak targeting to the nucleus and cytosol (Fig. 7D). These results collec-

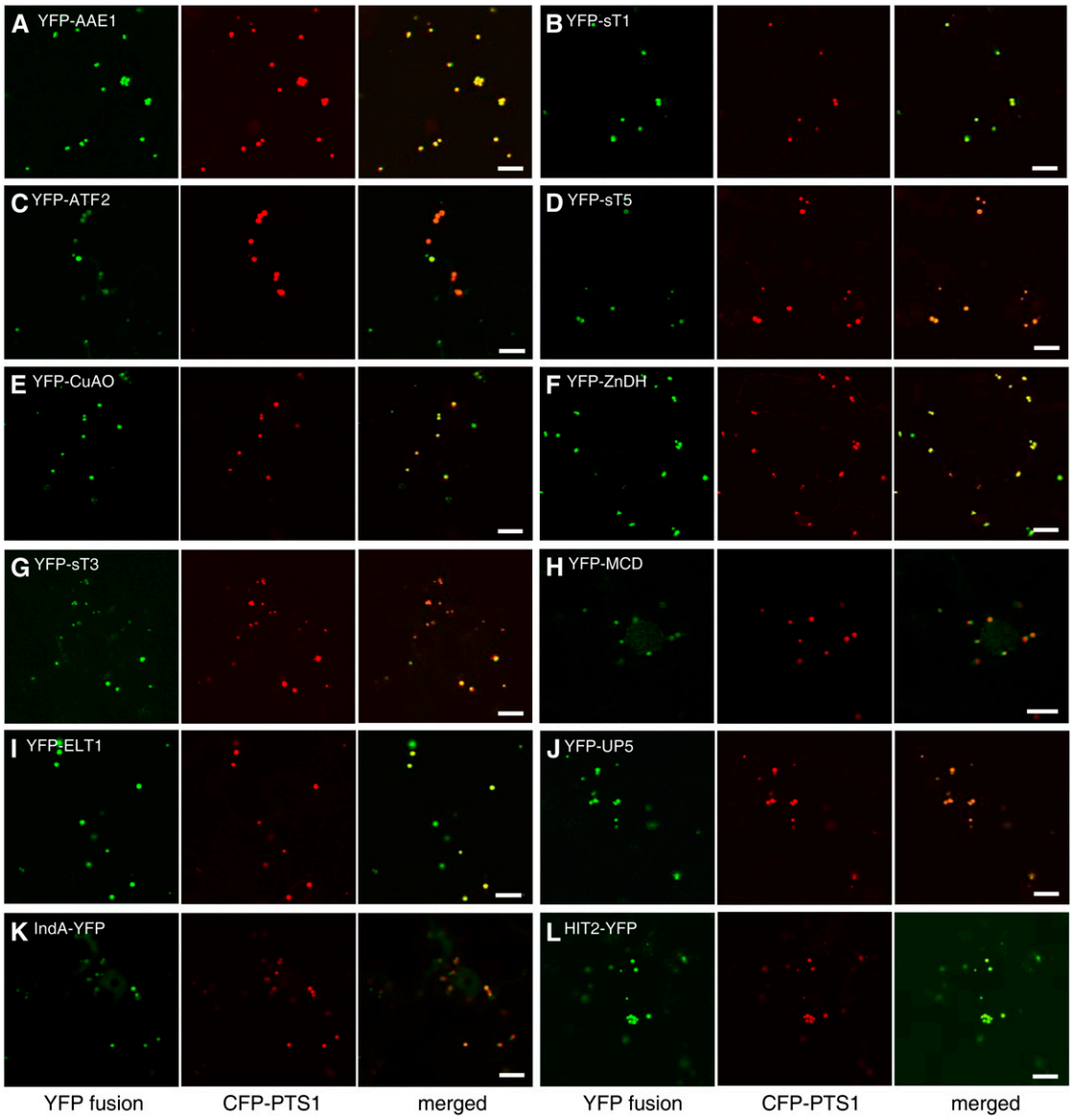

Figure 4. Peroxisomal localization of 12 proteins containing predicted PTSs. Confocal microscopic images were taken from leaf epidermal cells of 4-week-old tobacco plants in which YFP fusions and the *CFP-PTS1* peroxisomal marker were coexpressed. Bars = 10 μm.

tively demonstrated that an increasing number of peroxisomal proteins lacking predicted or closely related PTS1/2 tripeptides are being identified. These proteins may be either surface associated with or imported into peroxisomes via alternative yet unknown import mechanisms. However, peroxisome targeting of the remaining 12 proteins lacking obvious PTS-related sequences was not supported by our transient expression assays, as they were found to be associated with the nucleus, plasma membrane, or cytosol (Table II). These data suggest that (1) some proteins from this group could be contaminants from other compartments and (2) our transient expression system may have limitations in validating some of the true peroxisomal proteins.

DISCUSSION

Increasing the Dynamic Range of Protein Identification

A major goal of current plant peroxisomal proteome research is to detect low-abundance proteins by increasing the dynamic range of protein identification. This goal is challenging for leaf peroxisomes, because enzymes for the photorespiratory C_2 cycle and ROS detoxification predominate in leaf peroxisomes, constituting 63% of the total NSAF values of leaf peroxisomal proteins (Fig. 2C). These enzymes, together with the numerous enzymes related to fatty acid β-oxidation (another 23%), constitute nearly 90% of the leaf peroxisomal proteome (Fig. 2C). The predom-

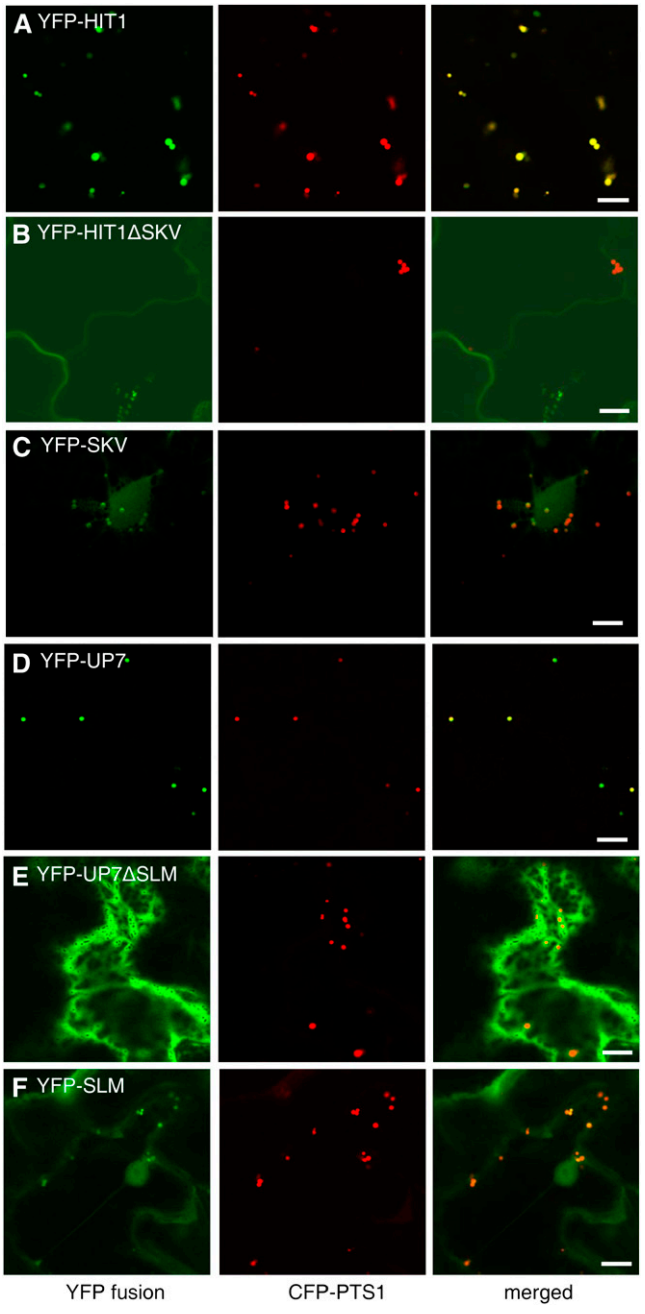

Figure 5. Identification of two novel PTS1 tripeptides, SKV> and SLM>. Confocal images were obtained from leaf epidermal cells of 4-week-old tobacco plants coexpressing the indicated YFP fusions and the *CFP-PTS1* peroxisomal marker. Bars = 10 μm.

inance of these matrix enzymes makes it difficult to identify by gel-based approaches novel peroxisomal proteins, especially those that have similar subunit molecular masses (30–60 kD), as the abundant proteins. In addition, the moderate abundance of leaf peroxisomes in mesophyll cells, their high fragility in aqueous solution, and their tight association in vivo with chloroplasts and mitochondria further limit the sensitivity of peroxisomal protein identifications and lead to minor, unavoidable copurification of mitochondria and chloroplasts with leaf peroxisomes. Using anti-VDAC immunoblotting and silver-stained gels for purity assessment, 1-DE, high-resolution HPLC separation of peptides, and high-sensitivity MS/MS, our study improved the dynamic range of protein identification and overcame these limitations to some degree.

The number of known and putative novel proteins identified as well as experimentally verified novel proteins of Arabidopsis peroxisomes in our study also surpasses those published for peroxisomes from fungi and mammals (for review, see Saleem et al., 2006), although a higher number of biogenesis proteins were identified in the mammalian peroxisome proteome study (Wiese et al., 2007). The same few PEX proteins were identified in our study and by Eubel et al. (2008), possibly reflecting the fact that Arabidopsis peroxisomes isolated from mature leaves and suspension cultured cells are less active in proliferation compared with those used for fungal and mammalian peroxisomal proteome analyses.

Among the five tested proteins with 98% or less probability of protein identification, two were confirmed to be peroxisomal (ATF2 and B12D1). These data, together with the fact that several known peroxisomal proteins were also identified by lower probability (Supplemental Table S2), demonstrate that some true positives could be identified from the group of proteins with slightly lower probability of protein identification.

The improved representation of hydrophobic and basic proteins by 1-DE, as opposed to 2-DE, enabled us to now detect several peroxisomal membrane proteins (Supplemental Table S2), the number of which is comparable to that identified by Eubel et al. (2008). However, the identification of other peroxisome membrane proteins, such as additional PEX proteins, will probably have to rely on further enrichment of peroxisomal membranes prior to proteomic analysis. In addition, we also identified some novel proteins that have a basic pI of greater than 9 and many small proteins (Table I; Supplemental Table S2) that may have precipitated or been insufficiently stained in 2-DE in previous proteome studies.

In summary, our in-depth proteome analysis represents a significant extension of protein identification from former studies (Fukao et al., 2002, 2003; Reumann et al., 2007; Arai et al., 2008; Eubel et al., 2008) and, in combination with in vivo subcellular targeting verifications, established 19 new peroxisomal proteins, to our knowledge, and thus markedly increased the number of matrix proteins discovered from plant peroxisomes (Fig. 8).

It was previously shown that NSAF quantification of proteins correlates well with gel-based quantification (Zybailov et al., 2008). However, it was also found that spectral counting tends to underestimate the amount of the most abundant proteins, such as cata-

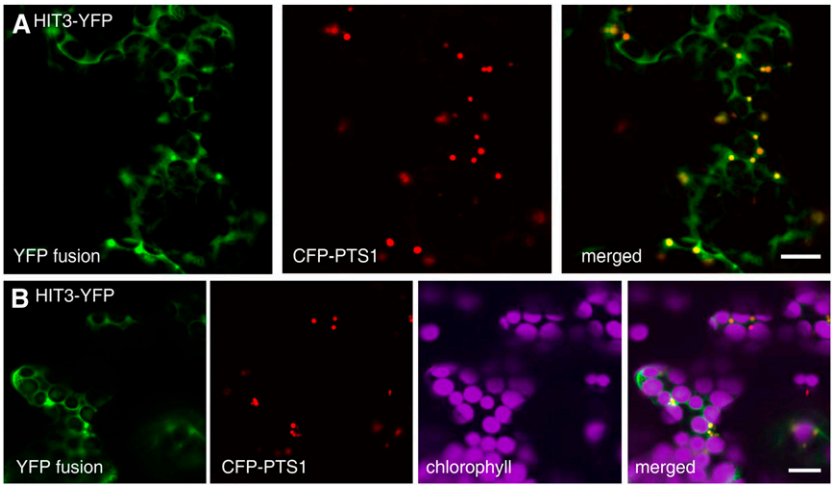

Figure 6. Dual localization of the HIT3 protein, which has an N-terminal PTS2-related sequence. Confocal images taken from leaf epidermal cells of 4-week-old tobacco plants coexpressing the indicated YFP fusion and the *CFP-PTS1* peroxisomal marker are shown. Bars = 10 μm.

lase in the case of peroxisomes, whereas gel-based quantification tends to be less accurate for low-abundance proteins (Zybailov et al., 2008). In addition, hydrophobic membrane proteins on average have fewer tryptic cleavage sites than hydrophilic soluble proteins. As a result, fewer peptides per protein are expected to be detected for membrane proteins than for soluble proteins, thus leading to a systematic underestimation of membrane protein abundance. Since the focus of our study was predominantly on the discovery of low-abundance peroxisomal proteins, we overloaded the protein gel before generating slices for tryptic digests, which may have also compromised NSAF-based quantification. Finally, our results were obtained from a single shotgun proteomic experiment with no replications, yet significant variations in spectral counts could be observed between independent experiments. Nevertheless, the NSAF-based protein quantification data presented in this study do represent a tentative indication of protein abundance in peroxisomes. Further targeted studies, including larger numbers of replicates, will be required for a detailed quantification of the peroxisomal proteome.

Annotation of Putative Novel Peroxisomal Proteins

The increased detection of nonperoxisomal proteins made our annotation of potential novel proteins more difficult. Notably, many of the proteins stringently classified here as plastidic or mitochondrial contaminants were identified only in the most recent and comprehensive proteome studies of chloroplasts and mitochondria (Kleffmann et al., 2004; Peltier et al., 2006; Heazlewood et al., 2007; Zybailov et al., 2008). It is possible, therefore, that some of these proteins are actually dual-targeted, true components of leaf peroxisomes. In future studies, the dual targeting issue can be addressed by in vivo localization analyses and differential proteome analyses comparing peroxisome isolates with different purities.

Intriguingly, most proteins designated as potential novel peroxisomal proteins lack computationally predictable targeting signals and have been tentatively annotated as cytosolic. The lack of predictable PTS1/2s in many novel proteins of peroxisomes is largely consistent with our current knowledge of the mechanisms and signals for protein targeting to peroxisomes. First, hydrophobic proteins, such as integral and peripheral proteins of the peroxisomal membrane, which are better covered by the 1-DE shotgun proteomic approach chosen here, lack PTS1/2 sequences. Second, accumulating evidence suggests that low-abundance matrix proteins preferentially carry unusual and mostly unknown variants of PTS peptides (Reumann et al., 2007; G. E. Antonicelli, T. Lingner, P. Meinicke, and S. Reumann, unpublished data). Supporting this idea is the in vivo peroxisome targeting confirmation for three proteins with PTS-related peptides and low NSAF values (Table I). Our confirmation of peroxisomal proteins carrying PTS-related peptides will contribute to the recognition of more functional PTS peptides and improve the prediction accuracy for low-abundance peroxisomal proteins in future proteome studies. In this regard, whole plants may be a more suitable peroxisome source for the identification of low-abundance and regulatory proteins, as novel PTS1/2s were not identified in the peroxisome proteome study of Arabidopsis cell suspension cultures (Eubel et al., 2008). Third, little is known about alternative import pathways for peroxisomal matrix proteins containing non-PTS1/2 targeting signals (with the exception of catalase). Confirmation of peroxisomal localization for four proteins lacking recognizable PTS clearly indicates novel import mechanisms. Peroxisomal localization was observed only when these four proteins were fused to the N terminus of YFP, whereas they remained cytosolic or showed no YFP fluorescence when fused to the C terminus of YFP (data not shown). As such, the above four proteins may contain novel N-terminal PTSs not yet recognized. B12D1, which has a hydrophobic domain in the N terminus (Table II), may be membrane attached to peroxisomes via this domain. In summary, our data suggest that the natural variability of PTS1/2 peptides

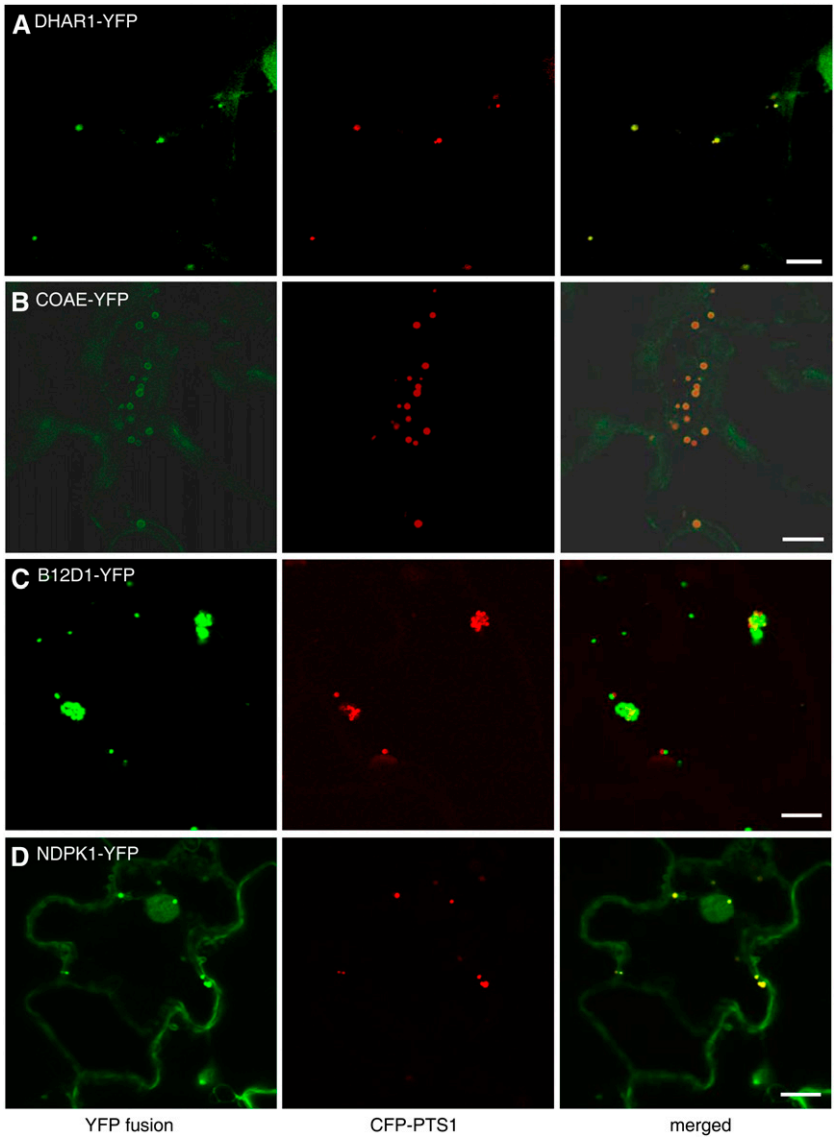

Figure 7. Peroxisomal localization of four novel proteins without predicted PTSs. Shown are confocal images taken from leaf epidermal cells of 4-week-old tobacco plants coexpressing the indicated YFP fusion proteins and *CFP-PTS1*. Bars = 10 μm.

and import pathways for peroxisomes are far from being completely understood.

In Vivo Targeting Analysis Verifies New Peroxisomal Proteins and Reveals Novel PTS Peptides

Using in vivo targeting analysis, we confirmed the peroxisomal association of 19 proteins identified by proteomics. We consider the terminal placement of the reporter protein well suited for conclusive subcellular targeting analyses. For instance, in YFP-X constructs, predicted PTS1 domains are in their native conformation with regard to the full-length protein (i.e. surface exposed or internally hidden). Creating "internal" fusions by inserting GFP 10 amino acids upstream from the C terminus (Eubel et al., 2008) may not be able to preserve native folding of the PTS1 domain in the reporter protein.

Our data have defined SLM> and SKV> as two novel plant PTS1s and suggested that the PTS2-related N-terminal nonapeptide RLx_5HF is a functional PTS2. SLM> is an unusual PTS1, as it contains a Leu residue at position −2, which is absent from all plant PTS1 tripeptides characterized to date. Plant PTS1 tripeptides have been shown previously to tolerate significant structural deviations from the general requirement of a positively charged residue at this position (Mullen et al., 1997; Kragler et al., 1998; Reumann et al., 2004, 2007). Most novel PTS1 tripeptides, such as SS[LI]>, ASL>, and SLM>, are generally found in low-abundance peroxisomal proteins (Reumann et al., 2007). The relatively pronounced cytosolic background fluorescence of YFP-SLM and YFP-SKV is consistent with the idea that these fairly weak PTS1s require targeting enhancer elements, such as R (position −4) in front of SLM> in UP7, to evoke peroxisome targeting. Notably, both tripeptides were fused directly to the C terminus of EYFP, which terminates with GMDELYK>, thus creating in the fusion protein a targeting enhancing Lys residue at

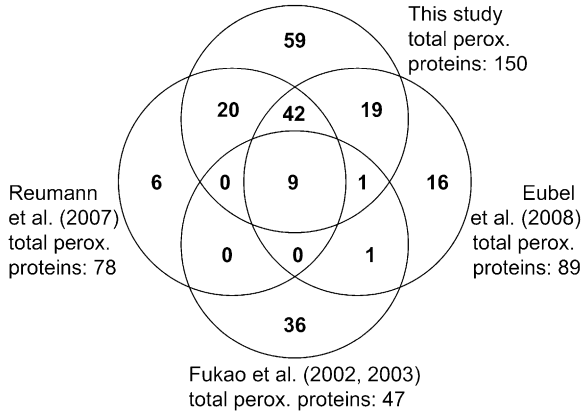

Figure 8. Comparison of Arabidopsis peroxisomal proteome data. The number of peroxisomal proteins identified in this study was compared with that from previous proteome studies by Reumann et al. (2007), Fukao et al. (2002, 2003), and Eubel et al. (2008). One protein is shared uniquely by Reumann et al. (2007) and Eubel et al. (2008) and could not be displayed on this Venn diagram.

position −4. Hence, these novel PTS1s by themselves are most likely weak PTS1 tripeptides and less efficient in targeting proteins to peroxisomes.

While transient protein expression in tobacco leaves is an ideal methodology for testing subcellular protein targeting in a high-throughput fashion, it may have some limitations. Although the 14 proteins that failed to show peroxisome targeting in our transient assay are possible contaminants from other cell compartments, some of them may be truly associated with peroxisomes in plant cells. For example, members of the 14-3-3 protein family (general growth factors [GRFs]) generally bind to phosphorylated proteins and regulate signal transduction by regulating the localization of the bound proteins (DeLille et al., 2001). GRF6 (14-3-3λ; Table I) interacts not only with components of the brassinolide signaling pathway, such as BZR1, in the cytosol (Srinivas et al., 2007) but also with the peroxisomal membrane-bound ascorbate peroxidase, APX3 (Yan et al., 2002). This result indicates the possible association of GRF6 with the peroxisome through binding of the cytosolic domain of APX3 and is consistent with the lack of a predicted PTS1/2 on this protein. Several other possible scenarios may exist for the failure of peroxisome targeting of some proteins using our tobacco system. First, the peroxisome targeting of some regulatory proteins may be highly regulated by exogenous and endogenous signals that are otherwise lacking in a standard transient expression system. In addition, many proteins are known to be synthesized from the same gene by alternative transcription and translation (Supplemental Table S3). Some protein variants identified by proteomics could be falsely assigned to the default gene model that is present in the databases, which may lack the correct PTS and consequently be nonperoxisomal in in vivo targeting assays. Finally, some peroxisomal proteins are unique to the Brassicaceae (Fig. 3; Supplemental Fig. S1) and therefore may require Brassicaceae-specific factors, which are lacking in *Nicotiana*, for targeting.

Extended β-Oxidation-Related Metabolism in Photosynthetic Tissue

The many proteins identified in this study and conclusively demonstrated to be peroxisome targeted in vivo suggest that leaf peroxisomes perform a wider range of metabolic functions than previously anticipated. One example is fatty acid β-oxidation-related metabolism. We identified a number of, to our knowledge, new auxiliary enzymes presumably involved in leaf peroxisomal β-oxidation. Besides the six known peroxisomal acyl-activating enzymes (AAEs), AAE1 and AAE17 belong to distinct clades of the AAE superfamily (Shockey et al., 2003). The three small thioesterases now verified to be peroxisome targeted (sT1, sT3, and sT5) are homologous to prokaryotic enzymes catabolizing phenylacetic acid and 4-Cl-benzoate (Reumann et al., 2004) and to human hTHEM2. The plant family members of sTs, all of which have yet unknown physiological functions, are apparently the only peroxisomal isoforms in eukaryotes. Conservation of those residues that presumably form the active site in human hTHEM2 (N50, H56, G57, and D65; Cheng et al., 2006) suggests conserved substrate specificity for some plant homologs (e.g. sT4 similar to hTHEM2; sT1 and sT2 similar to *Arthrobacter* species PaaI) and divergent substrate preferences for others (sT3, sT5, and sT6; Supplemental Fig. S2).

Malonyl-coenzyme A decarboxylase (MCD) catalyzes the breakdown of malonyl-CoA, an intermediate in fatty acid biosynthesis, to acetyl-CoA and carbon dioxide and is encoded by a single gene in Arabidopsis. The mammalian MCD is located in mitochondria, peroxisomes, and the cytoplasm (Sacksteder et al., 1999). Despite its predicted mitochondrial presequence, the Arabidopsis MCD protein has not been detected in the proteome of mitochondria or chloroplasts. This protein may be involved in the degradation of malonyl-CoA generated by β-oxidation of odd-chain-length dicarboxylic fatty acids and is exclusively peroxisomal in the Brassicaceae (Supplemental Fig. S1).

Polyamine Metabolism

Copper amine oxidases (CuAOs; EC 1.4.3.6) and flavin-containing amine oxidases catalyze the oxidative deamination of polyamines, ubiquitous compounds essential for cell growth and proliferation (Cona et al., 2006). The former require copper as a cofactor to oxidize a conserved Tyr residue at the catalytic site into a tropaquinone. Both copper amine and polyamine oxidases have been associated with peroxisomal metabolism in mammals (Wu et al., 2003) and predicted to reside in plant peroxisomes

(Reumann et al., 2004). Recombinant CuAO of tobacco, possibly peroxisome targeted by AKL>, has recently been characterized as a methylputrescine oxidase (MPO1; Heim et al., 2007). Arabidopsis CuAO, which we have now confirmed to be a leaf peroxisomal protein (Fig. 4E), is the closest homolog of tobacco MPO1 (83% sequence identity). These data strongly indicate that tobacco MPO1 is peroxisomal and that AtCuAO, the only Arabidopsis homolog with a predicted PTS, functions as an MPO.

A New Family of Nucleotide-Binding Proteins

HIT proteins constitute a superfamily of nucleotide-binding, -hydrolyzing, and -transfering enzymes, using the common motif His-x-His-x-His-xx (x being a hydrophobic residue) as the active catalytic site (Brenner, 2002). Animal HIT proteins such as Hint and Fhit are present in the nucleus, the cytosol, or mitochondria, hydrolyzing substrates such as AMP-NH_2, AMP-Lys, and diadenosinpolyphosphates (Ap_nA; n = 3 or 4; Huber and Weiske, 2008). Although the direct biological consequences of their catalytic activities are unclear, HIT proteins have been found to play crucial roles in tumorigenesis by regulating the function of transcription complexes and possibly other unidentified enzymes (Huber and Weiske, 2008).

In the Arabidopsis genome, we have found five HIT proteins encoded by At5g16566 (*HIT1*), At5g48545 (*HIT2*), At3g56490 (*HIT3*), At1g31160, and At5g58240. Our study conclusively identified three of them to be peroxisomal, all of which carry PTSs. Interestingly, *HIT2* was identified as one of the few genes upregulated in Arabidopsis stem explants treated with indole 3-butyric acid (IBA), an indole-3-acetic acid precursor that specifically promotes adventitious root formation (Ludwig-Müller et al., 2005). In peroxisomes, IBA is catabolized to the active auxin indole-3-acetic acid via a pathway analogous to fatty acid β-oxidation (Zolman et al., 2008). Therefore, it is tempting to speculate that HIT2 may be involved in the IBA β-oxidation pathway. The localization of HIT3 to the periphery of chloroplasts in addition to peroxisomes may indicate a dual function for this protein in metabolic pathways associated with both types of organelles. Although the substrates for HIT1, HIT2, and HIT3 remain to be identified, these three proteins represent a new class of plant enzymes whose functions are mainly associated with peroxisomes.

Two Kinases with Putative Regulatory Functions

Our confocal microscopic analysis suggests that the putative dephospho-CoA kinase, COAE, is possibly associated with the membrane of peroxisomes despite its lack of predicted transmembrane domains (Fig. 7B; Table II). Dephospho-CoA kinases catalyze the final step of CoA biosynthesis by phosphorylating the 3′-hydroxyl group of Rib, using ATP as a phosphate donor (Obmolova et al., 2001). Localization of COAE at the peroxisomal membrane suggests that this reaction is associated with either CoA recycling or peroxisomal activation of fatty acids by acyl-CoA synthetase.

Nucleoside diphosphate kinase catalyzes the transfer of a phosphate group from a nucleoside triphosphate, such as ATP, onto a nucleoside diphosphate, such as GDP, thereby converting one molecule of each GDP and ATP into GTP and ADP. By this reaction, NDPK controls the level of GTP, which is, for example, required for the conversion of inactive GDP-bound GTPases to the active GTP-bound form. NDPK2, another isoform of NDPK in Arabidopsis, was shown to bind and stimulate the GTPase activity of small G proteins and serve as a signal transducer in phytochrome signaling (Choi et al., 1999; Shen et al., 2008). Interestingly, it was previously shown that NDPK activity is required for dynamin-dependent endocytosis in *Drosophila* (Krishnan et al., 2001) and that the level of GTP-bound dynamin proteins controls the level of endocytosis (Sever et al., 2000). It is thus tempting to hypothesize that, by controlling the activation state of GTPases, NDPK1 might be associated with the control of peroxisome proliferation, shape, or biogenesis.

CONCLUSION

We have taken an important step toward defining a comprehensive protein map of plant peroxisomes. Next to the predominating enzymes involved in photorespiration and ROS metabolism, we can now detect a large number of peroxisomal proteins of moderate or even low abundance, among which are some regulatory proteins with unexpected peroxisome-related functions that had not been revealed by previous proteome studies of Arabidopsis peroxisomes. Confirmation of the peroxisome association of all of the putative novel proteins with in vivo targeting analysis or alternative methods is crucial before we can unequivocally further expand the current map of the peroxisome proteome. Mapping of the targeting signals on the novel proteins lacking predicted PTSs will provide important insights into yet unknown import pathways and transport mechanisms of matrix and membrane proteins of low abundance. Functional analyses of these novel proteins by reverse genetics should shed light on new metabolic and regulatory mechanisms and signal transduction cascades in peroxisomes.

MATERIALS AND METHODS

Plant Growth and Isolation of Leaf Peroxisomes

Arabidopsis (*Arabidopsis thaliana* ecotype Columbia) plants were grown for 4 to 6 weeks in a 16-h-light/8-h-dark cycle under 100 to 150 μE m^{-2} s^{-1} light. Rosette leaves were harvested and leaf peroxisomes isolated as described previously (Reumann et al., 2007). Protein concentration was determined as described before (Ma et al., 2006) using bovine serum albumin as a standard.

Postpreparative Purity Analysis by Immunoblotting

Proteins were precipitated by chloroform/methanol (Wessel and Flugge, 1984) and separated on minigels. For immunoblotting, we transferred proteins in a semidry system according to standard procedures. Arabidopsis VDAC was detected by a monoclonal antiserum against the maize (*Zea mays*) VDAC (provided by Thomas Elthon, University of Nebraska), followed by anti-mouse IgGs coupled to horseradish peroxidase, and was visualized by enhanced chemiluminescence. Silver staining of proteins was performed according to Blum et al. (1987). Based on anti-VDAC cross-reactivity, silver-staining intensity of the 110-kD P-protein band, and total protein visible by SDS-PAGE, leaf peroxisome isolates were classified into three categories: high, moderate, and low purity. Selected leaf peroxisome isolates of high purity were used as internal standards on all subsequent minigels.

1-DE LC-Electrospray Ionization-MS/MS

The proteins of highly pure Arabidopsis leaf peroxisomes (500 μg) were precipitated (Wessel and Flugge, 1984), dissolved in 80 μL of sample buffer, and loaded onto a single lane of a minigel for electrophoresis. After the protein front ran approximately 5 cm onto the resolving gel, the gel was faintly stained by Coomassie Brilliant Blue and cut into 16 slices, each of which was later digested by trypsin (Shevchenko et al., 1996).

The extracted peptides were automatically injected by a Waters nanoAcquity Sample Manager (www.waters.com) and loaded for 5 min onto a Waters Symmetry C18 peptide trap (5 μm, 180 μm $\times$ 20 mm) at 4 μL min^{-1} in 2% acetonitrile/0.1% formic acid. The bound peptides were then eluted onto a Waters BEH C18 nanoAcquity column (1.7 μm, 100 μm $\times$ 100 mm) and eluted over 120 min with a gradient of 5% B to 90% B in 103 min using a Waters nanoAcquity UPLC system (buffer A = 99.9% water/0.1% formic acid, buffer B = 99.9% acetonitrile/0.1% formic acid) into a ThermoFisher LTQ-FTICR mass spectrometer (www.thermo.com) at a flow rate of 300 nL min^{-1}. Survey scans were taken in the Fourier transformation at 25,000 resolution at a mass-to-charge ratio of 400, and the top 10 ions in each survey scan were then subjected to automatic low-energy collision-induced dissociation in the LTQ-FTICR mass spectrometer. The resulting MS/MS spectra were converted to peak lists using BioWorks Browser version 3.2 (ThermoFisher) with default parameters and searched using the Mascot searching algorithm version 2.2 (www.matrixscience.com) against the TAIR8 genome database downloaded from TAIR (http://www.Arabidopsis.org/). The Mascot output was then analyzed using Scaffold (www.proteomesoftware.com) to probabilistically validate protein identifications using the ProteinProphet (Nesvizhskii et al., 2003) computer algorithm. Protein-length-normalized NSAF values were calculated according to Paoletti et al. (2006).

Generation of Constructs

Two destination vectors were created using Gateway cloning technology (Invitrogen). Using the pPZP212 binary vector (Hajdukiewicz et al., 1994) as a backbone, the 35S promoter, hexa-His (6xHis), and YFP (Clontech) were sequentially cloned into the vectors. pDest-35S-6xHis-YFP-X was designed for fusion of genes with putative PTS1 signals to the C terminus of YFP; pDest-35S-X-YFP-6xHis was designed for fusing genes with putative PTS2 to the N terminus of YFP. The coding region of a novel peroxisomal gene was PCR amplified from the cDNA clone obtained from the Arabidopsis Biological Resource Center or from total RNA of ecotype Columbia seedlings. Each PCR product was first cloned into a donor vector (pDONR207) by the Gateway BP reaction to create an entry clone and later into the destination vector by the Gateway LR reaction (Invitrogen).

Transient Expression of cDNAs and CLSM

Four-week-old tobacco (*Nicotiana tabacum*) plants were used for the *Agrobacterium tumefaciens*-mediated transient expression assays. *A. tumefaciens* strains C85C1 and GV3101 (pMP90) containing the plasmid of interest were incubated at 28°C overnight, washed, and resuspended in water to an optical density at 600 nm of 0.5. Cells transformed with plasmids harboring either a YFP fusion or the CFP-PTS1 peroxisomal marker were mixed and infiltrated into tobacco leaves using 1-mL needleless syringes. Leaves of infiltrated plants were analyzed after 2 d by CLSM (Zeiss LSM 510 META). We used 458-, 514-, and 633-nm lasers to excite CFP, YFP, and chlorophyll, respectively. Fluorescence was detected using an emission filter of a 460- to 510-nm band pass for CFP, a 520- to 555-nm band pass for YFP, and a 650-nm long pass for chlorophyll. All images were acquired from single optical sections.

Supplemental Data

The following materials are available in the online version of this article.

Supplemental Figure S1. Analysis of PTS conservation in homologous plant ESTs for some of the peroxisomal proteins identified reproducibly by proteomics in this study.

Supplemental Figure S2. Sequence alignment of small thioesterase homologs.

Supplemental Table S1. Nonperoxisomal proteins identified in Arabidopsis leaf peroxisomes.

Supplemental Table S2. Sixty-five established proteins of plant peroxisomes identified in Arabidopsis leaf peroxisomes by 1-D LC-MS/MS.

Supplemental Table S3. Detailed biophysical and MS data for the proteins listed in Table I.

Supplemental Table S4. Arabidopsis proteins terminating with the novel PTS1 tripeptides SLM> and SKV>.

Supplemental Document S1. Abbreviations used in this report and plant species acronyms used in Figure 3 and Supplemental Figure S1.

ACKNOWLEDGMENTS

We thank the Arabidopsis Biological Resource Center for providing cDNA clones, Ethan Dawson-Baglien for technical assistance, and Karen Bird for editorial assistance.

Received February 25, 2009; accepted March 23, 2009; published March 27, 2009.

LITERATURE CITED

Aksam EB, Koek A, Kiel JA, Jourdan S, Veenhuis M, van der Klei IJ (2007) A peroxisomal Lon protease and peroxisome degradation by autophagy play key roles in vitality of Hansenula polymorpha cells. Autophagy **3:** 96–105

Arai Y, Hayashi M, Nishimura M (2008) Proteomic analysis of highly purified peroxisomes from etiolated soybean cotyledons. Plant Cell Physiol **49:** 526–539

Beevers H (1979) Microbodies in higher plants. Annu Rev Plant Physiol **30:** 159–193

Blum H, Beier H, Gross HJ (1987) Improved silver staining of plant proteins, RNA and DNA in polyacrylamide gels. Electrophoresis **8:** 93–99

Brenner C (2002) Hint, Fhit, and GalT: function, structure, evolution, and mechanism of three branches of the histidine triad superfamily of nucleotide hydrolases and transferases. Biochemistry **41:** 9003–9014

Brocard C, Hartig A (2006) Peroxisome targeting signal 1: is it really a simple tripeptide? Biochim Biophys Acta **1763:** 1565–1573

Cheng Z, Bao S, Shan X, Xu H, Gong W (2006) Human thioesterase superfamily member 2 (hTHEM2) is co-localized with beta-tubulin onto the microtubule. Biochem Biophys Res Commun **350:** 850–853

Choi G, Yi H, Lee J, Kwon YK, Soh MS, Shin B, Luka Z, Hahn TR, Song PS (1999) Phytochrome signaling is mediated through nucleoside diphosphate kinase 2. Nature **401:** 610–613

Cona A, Rea G, Angelini R, Federico R, Tavladoraki P (2006) Functions of amine oxidases in plant development and defence. Trends Plant Sci **11:** 80–88

DeLille JM, Sehnke PC, Ferl RJ (2001) The Arabidopsis 14-3-3 family of signaling regulators. Plant Physiol **126:** 35–38

Desai M, Hu J (2008) Light induces peroxisome proliferation in Arabidopsis seedlings through the photoreceptor phytochrome A, the transcription factor HY5 HOMOLOG, and the peroxisomal protein PEROXIN11b. Plant Physiol **146:** 1117–1127

Emanuelsson O, Elofsson A, von Heijne G, Cristobal S (2003) In silico

prediction of the peroxisomal proteome in fungi, plants and animals. J Mol Biol **330:** 443–456

Eubel H, Meyer EH, Taylor NL, Bussell JD, O'Toole N, Heazlewood JL, Castleden I, Small I, Smith SM, Millar AH (2008) Novel proteins, putative membrane transporters, and an integrated metabolic network are revealed by quantitative proteomic analysis of Arabidopsis cell culture peroxisomes. Plant Physiol **148:** 1809–1829

Fan J, Quan S, Orth T, Awai C, Chory J, Hu J (2005) The Arabidopsis PEX12 gene is required for peroxisome biogenesis and is essential for development. Plant Physiol **139:** 231–239

Fukao Y, Hayashi M, Hara-Nishimura I, Nishimura M (2003) Novel glyoxysomal protein kinase, GPK1, identified by proteomic analysis of glyoxysomes in etiolated cotyledons of Arabidopsis thaliana. Plant Cell Physiol **44:** 1002–1012

Fukao Y, Hayashi M, Nishimura M (2002) Proteomic analysis of leaf peroxisomal proteins in greening cotyledons of Arabidopsis thaliana. Plant Cell Physiol **43:** 689–696

Hajdukiewicz P, Svab Z, Maliga P (1994) The small, versatile pPZP family of Agrobacterium binary vectors for plant transformation. Plant Mol Biol **25:** 989–994

Hayashi M, Aoki M, Kondo M, Nishimura M (1997) Changes in targeting efficiencies of proteins to plant microbodies caused by amino acid substitutions in the carboxy-terminal tripeptide. Plant Cell Physiol **38:** 759–768

Hayashi M, Nishimura M (2003) Entering a new era of research on plant peroxisomes. Curr Opin Plant Biol **6:** 577–582

Heazlewood JL, Millar AH (2006) Plant proteomics: challenges and resources. *In* C Finnie, ed, Plant Proteomics. Blackwell Publishing, Oxford, pp 1–24

Heazlewood JL, Verboom RE, Tonti-Filippini J, Small I, Millar AH (2007) SUBA: the Arabidopsis Subcellular Database. Nucleic Acids Res **35:** D213–D218

Heim WG, Sykes KA, Hildreth SB, Sun J, Lu RH, Jelesko JG (2007) Cloning and characterization of a Nicotiana tabacum methylputrescine oxidase transcript. Phytochemistry **68:** 454–463

Hu J, Aguirre M, Peto C, Alonso J, Ecker J, Chory J (2002) A role for peroxisomes in photomorphogenesis and development of Arabidopsis. Science **297:** 405–409

Huber O, Weiske J (2008) β-Catenin takes a HIT. Cell Cycle **7:** 1326–1331

Jimenez A, Hernandez JA, Del Rio LA, Sevilla F (1997) Evidence for the presence of the ascorbate-glutathione cycle in mitochondria and peroxisomes of pea leaves. Plant Physiol **114:** 275–284

Kamada T, Nito K, Hayashi H, Mano S, Hayashi M, Nishimura M (2003) Functional differentiation of peroxisomes revealed by expression profiles of peroxisomal genes in *Arabidopsis thaliana*. Plant Cell Physiol **44:** 1275–1289

Kikuchi M, Hatano N, Yokota S, Shimozawa N, Imanaka T, Taniguchi H (2004) Proteomic analysis of rat liver peroxisome: presence of peroxisome-specific isozyme of Lon protease. J Biol Chem **279:** 421–428

Kleffmann T, Russenberger D, von Zychlinski A, Christopher W, Sjolander K, Gruissem W, Baginsky S (2004) The Arabidopsis thaliana chloroplast proteome reveals pathway abundance and novel protein functions. Curr Biol **14:** 354–362

Kragler F, Lametschwandtner G, Christmann J, Hartig A, Harada JJ (1998) Identification and analysis of the plant peroxisomal targeting signal 1 receptor NtPEX5. Proc Natl Acad Sci USA **95:** 13336–13341

Krishnan KS, Rikhy R, Rao S, Shivalkar M, Mosko M, Narayanan R, Etter P, Estes PS, Ramaswami M (2001) Nucleoside diphosphate kinase, a source of GTP, is required for dynamin-dependent synaptic vesicle recycling. Neuron **1:** 197–210

Lin Y, Sun L, Nguyen LV, Rachubinski RA, Goodman HM (1999) The Pex16p homolog SSE1 and storage organelle formation in Arabidopsis seeds. Science **284:** 328–330

Lipka V, Dittgen J, Bednarek P, Bhat R, Wiermer M, Stein M, Landtag J, Brandt W, Rosahl S, Scheel D, et al (2005) Pre- and postinvasion defenses both contribute to nonhost resistance in Arabidopsis. Science **310:** 1180–1183

Lisenbee CS, Lingard MJ, Trelease RN (2005) Arabidopsis peroxisomes possess functionally redundant membrane and matrix isoforms of monodehydroascorbate reductase. Plant J **43:** 900–914

Ludwig-Müller J, Vertocnik A, Town CD (2005) Analysis of indole-3-butyric acid-induced adventitious root formation on Arabidopsis stem segments. J Exp Bot **56:** 2095–2105

Ma C, Haslbeck M, Babujee L, Jahn O, Reumann S (2006) Identification and characterization of a stress-inducible and a constitutive small heat-shock protein targeted to the matrix of plant peroxisomes. Plant Physiol **141:** 47–60

Ma C, Reumann S (2008) Improved prediction of peroxisomal PTS1 proteins from genome sequences based on experimental subcellular targeting analyses as exemplified for protein kinases from Arabidopsis. J Exp Bot **59:** 3767–3779

Mullen RT, Lee MS, Flynn CR, Trelease RN (1997) Diverse amino acid residues function within the type 1 peroxisomal targeting signal: implications for the role of accessory residues upstream of the type 1 peroxisomal targeting signal. Plant Physiol **115:** 881–889

Nesvizhskii AI, Keller A, Kolker E, Aebersold R (2003) A statistical model for identifying proteins by tandem mass spectrometry. Anal Chem **75:** 4646–4658

Nyathi Y, Baker A (2006) Plant peroxisomes as a source of signalling molecules. Biochim Biophys Acta **1763:** 1478–1495

Obmolova G, Teplyakov A, Bonander N, Eisenstein E, Howard AJ, Gilliland GL (2001) Crystal structure of dephospho-coenzyme A kinase from Haemophilus influenzae. J Struct Biol **136:** 119–125

Olsen LJ, Harada J (1995) Peroxisomes and their assembly in higher plants. Annu Rev Plant Biol **46:** 123–146

Paoletti AC, Parmely TJ, Tomomori-Sato C, Sato S, Zhu D, Conaway RC, Conaway JW, Florens L, Washburn MP (2006) Quantitative proteomic analysis of distinct mammalian Mediator complexes using normalized spectral abundance factors. Proc Natl Acad Sci USA **103:** 18928–18933

Peltier JB, Cai Y, Sun Q, Zabrouskov V, Giacomelli L, Rudella A, Ytterberg AJ, Rutschow H, van Wijk KJ (2006) The oligomeric stromal proteome of *Arabidopsis thaliana* chloroplasts. Mol Cell Proteomics **5:** 114–133

Purdue PE, Lazarow PB (2001) Peroxisome biogenesis. Annu Rev Cell Dev Biol **17:** 701–752

Reumann S (2004) Specification of the peroxisome targeting signals type 1 and type 2 of plant peroxisomes by bioinformatics analyses. Plant Physiol **135:** 783–800

Reumann S, Babujee L, Ma C, Wienkoop S, Siemsen T, Antonicelli GE, Rasche N, Luder F, Weckwerth W, Jahn O (2007) Proteome analysis of *Arabidopsis* leaf peroxisomes reveals novel targeting peptides, metabolic pathways, and defense mechanisms. Plant Cell **19:** 3170–3193

Reumann S, Ma C, Lemke S, Babujee L (2004) AraPerox: a database of putative Arabidopsis proteins from plant peroxisomes. Plant Physiol **136:** 2587–2608

Reumann S, Weber AP (2006) Plant peroxisomes respire in the light: some gaps of the photorespiratory C2 cycle have become filled—others remain. Biochim Biophys Acta **1763:** 1496–1510

Sacksteder KA, Morrell JC, Wanders RJ, Matalon R, Gould SJ (1999) MCD encodes peroxisomal and cytoplasmic forms of malonyl-CoA decarboxylase and is mutated in malonyl-CoA decarboxylase deficiency. J Biol Chem **274:** 24461–24468

Saleem RA, Smith JJ, Aitchison JD (2006) Proteomics of the peroxisome. Biochim Biophys Acta **1763:** 1541–1551

Schumann U, Wanner G, Veenhuis M, Schmid M, Gietl C (2003) AthPEX10, a nuclear gene essential for peroxisome and storage organelle formation during Arabidopsis embryogenesis. Proc Natl Acad Sci USA **100:** 9626–9631

Sever S, Damke H, Schmid SL (2000) Dynamin: GTP controls formation of constricted coated pits, the rate limiting step in clathrin-mediated endocytosis. J Cell Biol **150:** 1137–1147

Shen Y, Han YJ, Kim JI, Song PS (2008) Arabidopsis nucleoside diphosphate kinase-2 as a plant GTPase activating protein. BMB Rep **41:** 645–650

Shevchenko A, Wilm M, Vorm O, Mann M (1996) Mass spectrometric sequencing of proteins silver-stained polyacrylamide gels. Anal Chem **68:** 850–858

Shockey JM, Fulda MS, Browse J (2003) Arabidopsis contains a large superfamily of acyl-activating enzymes: phylogenetic and biochemical analysis reveals a new class of acyl-coenzyme A synthetases. Plant Physiol **132:** 1065–1076

Sparkes IA, Brandizzi F, Slocombe SP, El-Shami M, Hawes C, Baker A (2003) An Arabidopsis *pex10* null mutant is embryo lethal, implicating peroxisomes in an essential role during plant embryogenesis. Plant Physiol **133:** 1809–1819

Srinivas SG, Kim TW, He J, Tang W, Deng Z, Bai M, Guan S, Lalonde S,

Sun Y, Gendron JM, et al (2007) An essential role for 14-3-3 proteins in brassinosteroid signal transduction in Arabidopsis. Dev Cell **13:** 177–189

Van den Bosch H, Schutgens R, Wanders R, Tager J (1992) Biochemistry of peroxisomes. Annu Rev Biochem **61:** 151–197

Wessel D, Flugge UI (1984) A method for the quantitative recovery of protein in dilute solution in the presence of detergents and lipids. Anal Biochem **138:** 141–143

Wiese S, Gronemeyer T, Ofman R, Kunze M, Grou CP, Almeida JA, Eisenacher M, Stephan C, Hayen H, Schollenberger L, et al (2007) Proteomics characterization of mouse kidney peroxisomes by tandem mass spectrometry and protein correlation profiling. Mol Cell Proteomics **6:** 2045–2057

Wu T, Yankovskaya V, McIntire WS (2003) Cloning, sequencing, and heterologous expression of the murine peroxisomal flavoprotein, N1-acetylated polyamine oxidase. J Biol Chem **278:** 20514–20525

Yan J, Wang J, Zhang H (2002) An ankyrin repeat-containing protein plays a role in both disease resistance and antioxidation metabolism. Plant J **29:** 193–202

Zolman BK, Martinez N, Millius A, Adham AR, Bartel B (2008) Identification and characterization of Arabidopsis indole-3-butyric acid response mutants defective in novel peroxisomal enzymes. Genetics **180:** 237–251

Zolman BK, Yoder A, Bartel B (2000) Genetic analysis of indole-3-butyric acid responses in *Arabidopsis thaliana* reveals four mutant classes. Genetics **156:** 1323–1337

Zybailov B, Rutschow H, Friso G, Rudella A, Emanuelsson O, Sun Q, van Wijk KJ (2008) Sorting signals, N-terminal modifications and abundance of the chloroplast proteome. PLoS One **3:** e1994